



**HAL**  
open science

# Experimental investigation of flammability and numerical study of combustion of shrub of rockrose under severe drought conditions

Frédéric Morandini, P.A. Santoni, J.B. Tramoni, W.E. Mell

► **To cite this version:**

Frédéric Morandini, P.A. Santoni, J.B. Tramoni, W.E. Mell. Experimental investigation of flammability and numerical study of combustion of shrub of rockrose under severe drought conditions. *Fire Safety Journal*, 2019, 108, pp.102836. 10.1016/j.firesaf.2019.102836 . hal-02171669

**HAL Id: hal-02171669**

**<https://hal.science/hal-02171669>**

Submitted on 25 Oct 2021

**HAL** is a multi-disciplinary open access archive for the deposit and dissemination of scientific research documents, whether they are published or not. The documents may come from teaching and research institutions in France or abroad, or from public or private research centers.

L'archive ouverte pluridisciplinaire **HAL**, est destinée au dépôt et à la diffusion de documents scientifiques de niveau recherche, publiés ou non, émanant des établissements d'enseignement et de recherche français ou étrangers, des laboratoires publics ou privés.



Distributed under a Creative Commons Attribution - NonCommercial 4.0 International License

# 1 **Experimental investigation of flammability and numerical study of** 2 **combustion of shrub of rockrose under severe drought conditions**

3 F. Morandini<sup>a</sup>, P.A. Santoni<sup>a</sup>, J.B. Tramoni<sup>a</sup>, W.E. Mell<sup>b</sup>

4 <sup>a</sup>Université de Corse CNRS UMR 6134 SPE, Campus Grimaldi, BP 52, 20250 Corte, France

5 <sup>b</sup>Pacific Wildland Fire Science Laboratory, U.S. Forest Service, 400 N 34<sup>th</sup> Street, Suite 201,  
6 Seattle, WA 98103, USA

7

## 8 **Abstract**

9 Structure of vegetation significantly influences its flammability and resulting fire spread.  
10 Despite considerable amount of laboratory studies, experimental works carried out with full  
11 plant specimens, representative of field conditions, are still limited. Present study aims to collect  
12 meaningful experimental data on structure and flammability of shrub of rockrose and evaluate  
13 the predictions of a fire model (WFDS) against this dataset. Spatial distribution of fuel elements,  
14 sorted according to their characteristic thickness, was established from destructive  
15 measurements. 28 fire tests were conducted with full plants under a calorimeter. Foliar moisture  
16 content was in the range of 4-18% on dry basis. Radiant panels were used as source of ignition.  
17 Flammability was investigated using ignitability, sustainability, combustibility and  
18 consumability. Comparison to previous studies highlighted the necessity of standardization  
19 among test procedures. Principal component analysis revealed four flammability regimes  
20 depending on proportion of thin fuel elements within the crown, position of ignition and  
21 duration of preheating. Finally, combustion dynamics of a shrub was numerically investigated  
22 with WFDS. A bulk density model was developed from the characterization study and used as  
23 input data for the numerical code. Predicted HRR was in good agreement with experiments,  
24 although simulation results need improvement in initiation phase of burning.

25

26 **Keywords:** Wildland fires; shrub flammability; Ignitability; Sustainability; Combustibility;  
27 Consumability; Mediterranean vegetation; Oxygen Consumption Calorimetry; WFDS.

28

## 29        **1. Introduction**

30        Large and severe wildfires have increased in occurrence, duration and intensity the last  
31 decade [1]. In 2017, these fires burnt over 1.2 and 4.1 million ha of natural lands in Europe [2]  
32 and United States [3], respectively, causing the worst wildfire season on record in many  
33 counties across the world. They caused billions of euros in damages and fire suppression costs  
34 and killed hundreds of people among fire fighters and civilians. The last catastrophic events  
35 that occurred in Portugal in 2017, and in Greece and California in 2018 have sadly confirmed  
36 this tendency. Continuous efforts are being made towards the understanding of the behavior of  
37 fires at several observation scales (laboratory experiments and field scale observations), the  
38 improvement of fire spread models of all types (statistical, semi-empirical, physical or detailed)  
39 and the development of decision support tools for fire management.

40        Vegetation plays a critical role in wildfire spread. Thus, flammability [4-6] of natural fuels  
41 is a fundamental aspect to identify potential fire impacts and hazards. It is defined as a  
42 combination of four inter-correlated components involving several material and related  
43 combustion properties. These components refer to the ability of vegetation to ignite  
44 (ignitability), to maintain combustion and produce energy during its thermal degradation  
45 (sustainability), to the rate of combustion (combustibility) and to the proportion of biomass  
46 consumed (consumability). The first two components of flammability are basically temporal  
47 measurements and are easy to evaluate. Thus, ignitability is often defined as the time to ignition  
48 [4, 7-9]. Sustainability is usually described as the flame duration [8-11]. The last two  
49 components involve combustion metrics and are less straightforward to measure, depending on  
50 the technique used. Metrics of various kind, such as flame temperature [8, 12], flame height [9,  
51 12, 13], rate of fire spread [7, 8] or rate of heat release [9, 11] were used as indicator for  
52 combustibility. Finally, the consumability has been characterized by the fuel consumption ratio,  
53 the residual mass fraction [7, 9, 12] or the mass loss rate [9, 11, 12]. It should be noticed that  
54 the whole four components are rarely used together to classify the flammability of natural fuels  
55 and ignition properties are often only considered [14, 15].

56        Flammability is difficult to evaluate since it is not a direct measurable property but a broad  
57 concept encompassing several metrics. Unlike for testing building materials, flammability of  
58 vegetation can be subject to debate [16] and some authors developed alternative frameworks  
59 [17-20]. No standardized procedure exists for evaluating the four components of flammability  
60 for natural fuels [9] and different metrics can be used to quantify a same component. For

61 instance, flame duration (in terms of visual flaming or duration above a threshold of  
62 temperature, heat release rate or radiant heat flux), heat of combustion or total heat released or  
63 surface area burnt can be used as indicators of sustainability [9]. More questionable is the use  
64 of the same metric for the evaluation of different flammability components. In particular, the  
65 mass loss rate during combustion was used as descriptor for consumability and combustibility  
66 [18, 21], and surface area burnt for sustainability and consumability [9, 18]. Many studies have  
67 emphasized the effects of fuel moisture content and fuel geometry on flammability [12, 14, 22-  
68 33]. The flammability was also shown to be scale dependent [9, 17, 18, 22, 31, 34]. However,  
69 the conditions of the assessment tests are frequently not representative of the ones encountered  
70 during wildfires [35]. The flammability tests are usually performed on isolated fuel particles  
71 (foliage, needles, litter, twigs, bark...) [14, 15, 33, 36-38] or plant parts (leafy branch) [19, 21,  
72 39, 40] but no relation with the full-plant flammability is provided. White and Zipperer [9]  
73 pointed out a lack of good documentation of the behavior of individual plants in natural fires.  
74 Indeed, burning characteristics of full-scale plant, characteristic of the field conditions, has  
75 received little attention [13, 22, 31, 41-53].

76 Bench scale calorimeters (cone, fire propagation apparatus, mass loss calorimeter) are  
77 usually used to estimate flammability of particular fuel elements or part of plants in the  
78 laboratory [22, 33, 37, 39, 54-57]. Such calorimeters have been developed for the study of  
79 building materials on a plane surface area basis and some difficulties occur when testing the  
80 porous fuel comprising plant parts. Furthermore, the sample holder modifies the back face  
81 boundary condition and the air inflow. This can significantly influence the burning behavior of  
82 the samples [54-59]. Contrary to micro-scale differential scanning calorimetry (DSC) or  
83 thermogravimetric analysis (TGA), where samples are reduced into uniform fine powder solid  
84 fuel (losing the link to the structure of the original material), bench scale calorimeters allow to  
85 assess the flammability of parts of plant (needles, leaves, twigs) with a heating rate  
86 representative of fire conditions in the open. However, the manual arrangement of the samples  
87 of vegetation used for fire tests at bench scale (litters, plant parts) alters the structure of these  
88 natural fuels. Indeed, the reconstruction of the vegetation layer modifies both its compactness  
89 and bulk density [60]. These changes influence ventilation within the fuel layer and resulting  
90 fire behavior [61, 62]. Consequently, the relationship between bench scale results on plant parts  
91 and flammability of the whole plant still needs to be addressed, making even more difficult to  
92 extend these tests to field fire scenarios.

93 The plant geometry, structure and composition (leaves, twigs of various diameters) were  
94 already identified as primary parameters determining its flammability [16, 35, 63-66].  
95 Experimental studies have also shown the effects of the size and spacing of fuel elements during  
96 fire tests [47, 66-70]. The particles of various kind and size, that compose the vegetation,  
97 participate in different ways in the combustion mechanisms that occur during fire spread.  
98 Typically, only fuel elements smaller than 6 mm in diameter contribute to the fire behavior  
99 [71]. The thinner the particles, the sooner they are involved in the thermal degradation processes  
100 [11, 36, 38]. Indeed, the leaves, needles or twigs (thickness  $\leq 2$  mm) are very prone to heating  
101 via convective heating and direct flame contact [72]. An increase in the proportion of overall  
102 fuel mass that is thin fuel elements was shown to result in the increase of both energy content  
103 [13] and proportion of fuel burnt [73].

104 Considering the difficulties with establishing relationships between heat release for the  
105 individual parts and the whole plant, the use of calorimetry measurements at full-scale seems a  
106 suitable alternative [9]. Few studies [13, 22, 31, 41-51, 53] were conducted to measure the  
107 burning characteristics for whole plants. The majority focused on some specific components of  
108 the flammability. The measurements of the burning characteristics performed on full scale  
109 plants are synthesized in Table 1 and are expressed in relation to flammability components.  
110 Some of these studies used calorimetry to provide the measurement of the Heat Release Rate  
111 (HRR) which is among the most important parameters for understanding flammability,  
112 characterizing fire hazard and ranking fuels [74]. This fundamental property can also be used  
113 to estimate potential for ignition of adjacent fuel elements along with emitted radiant heat flux.  
114 The main difference between fire tests carried out at bench scale and full scale is that the natural  
115 structure of the vegetation is kept intact in the latter. Furthermore, the flame spread across the  
116 whole plant is taken into account [20, 44]. The comparison of results collected at different scales  
117 is a complex task [11]. Experiments carried out on the same fuels at different scales showed  
118 contradictory conclusions. While some authors measured a reasonable agreement between both  
119 scales [75] others obtained either an increase of peak HRR with increasing scale [22] or the  
120 opposite outcome [11, 59]. Moreover, considering the wide range of sample conditioning (fuel  
121 elements, parts of plants, full-scale plants), ignition method (radiant source, flame) and fire test  
122 conditions (still air or wind to favor combustion), the evaluation of the flammability  
123 components is highly dependent of the experimental procedure. As a result, differences in fire  
124 behavior can be related to the experimental setup rather than vegetation characteristics.

125 Fire experiments were reported to offer a limited insight into vegetation-fire dynamics  
126 interactions and physics-based fire spread models were suggested to be the best way for  
127 understanding plant flammability [35]. Numerical simulations, based on computational fluid  
128 dynamics [30, 76-83], have been extensively used to improve the knowledge of fire spread  
129 across vegetation at various scales and could have practical applications in fire and landscape  
130 managements. These models need to be compared over a wide range of configurations for sub-  
131 models improvement purposes. In particular, the Wildland-urban interface Fire Dynamics  
132 Simulator (WFDS) was tested at field scale with large experimental grassland fires [83].  
133 However, this first modelling approach considered only a boundary fuel model. Next, the spatial  
134 distribution of different fuel elements (leaves, twigs) within a vegetation layer was implemented  
135 [80], but char combustion processes was nevertheless not considered at this stage. Further  
136 improvements have consisted in the modification of the thermal degradation sub-model in order  
137 to include the char oxidation, the refinement of the gasification law [79]. The predictions were  
138 in a satisfactory agreement with the experimental data on fire spread across pine needle beds.

139 The present study focusses on the experimental and numerical investigations of the  
140 flammability of single shrubs of rockrose. The first aim is to characterize the distribution of the  
141 fuel elements (leaves and twigs of various diameters ranked by size classes) within the shrub.  
142 From these experimental data, the distribution of each class of particles is estimated. The  
143 resulting bulk density is then used as input for WFDS. The second aim is to assess the shrub  
144 flammability based on the four components (ignitability, sustainability, combustibility and  
145 consumability). The fire tests were conducted with dried shrubs with unmodified structure  
146 submitted to an external heat flux (radiation alone), providing a flammability measurement  
147 much closer to that of individuals in the field than those obtained from parts of plants. An  
148 originality of the work lies in the measurements of HRR (by oxygen consumption calorimetry)  
149 and fuel consumption at particle level (from destructive sampling of burned shrubs) as  
150 indicators of the shrub combustibility and consumability, respectively. The predictions of  
151 WFDS are then evaluated against this dataset in order to test this model and highlight future  
152 improvement directions.

153

## 154 2. Material and Methods

### 155 2.1. Vegetation characterization

156 Accurate vegetation characterization is required to assess the flammability of complex  
157 fuel such as shrub. The present work focuses on shrubs of rockrose (*Cistus monspeliensis*), an  
158 abundant vegetation of the Mediterranean basin, typical of maquis, that is frequently involved  
159 in wildland fires. This pyrophytic species is known for his level of invasiveness in these areas,  
160 particularly in Corsica where the study is conducted. Furthermore, the shrub of rockrose has a  
161 large seasonal variability of moisture content of live fine fuel [32]. Consequently, it is difficult  
162 to eliminate outside of the fire season using prescribed burnings since they are conducted under  
163 very high foliar moisture content conditions (>200%) that result in marginal burning.  
164 Paradoxically during summer, it generates high intensity fires, hard to suppress and often  
165 responsible of firefighters fatalities in steep slope and wind conditions [84, 85]. Indeed, for  
166 small shrubs, moisture content can decrease during this season down to values lower than 20%  
167 [86] and thus these plants reach an even higher fire hazard when period of intense droughts  
168 occurs. The shrub of rockrose is composed of fuel elements of different size distributed non  
169 uniformly. From top to bottom the shrub is composed of a crown containing leaves and small  
170 twigs, an intermediate part mainly formed of twigs of several diameters and a base made of  
171 largest fuel elements. As a first step toward a better understanding of the fire spread mechanisms  
172 across shrublands, a characterization study of the shrubs of rockrose was performed.  
173 Measurements of the shrub structure (proportion and 3D spatial distribution of fuel particles of  
174 different kind and size) were carried out on three shrubs harvested in central region of Corsica,  
175 France (42°17'N, 9°10'E) during autumn. The base of the rockroses composed of large fuel  
176 elements was not considered in this study. Such large diameter twigs (>25 mm in diameter)  
177 don't participate in the dynamics of fire spread although they could be thermally degraded and  
178 burned after long exposure within the fire front, depending on fire intensity. The plants were  
179 harvested in the same vegetation plot and were chosen to be approximately the same size and  
180 relatively uniform in shape. They were cut off a few centimeters above the ground. The average  
181 ( $\pm$  standard deviation) height of the samples of rockrose was  $1.23 \pm 0.12$  m. The average crown  
182 depth and diameter (measured at mid-crown height) were  $0.35 \pm 0.07$  m and  $0.68 \pm 0.06$  m,  
183 respectively. The overall shrub mass (excluding the bottom of the base attached to the roots),  
184 on live and dry basis, were  $1.30 \pm 0.28$  kg and  $0.76 \pm 0.03$  kg, respectively. In order to determine  
185 qualitatively and quantitatively the different fuel elements constituting this shrub species, a  
186 sampling was performed at particle level according to the cube method [15, 87, 88], which

187 allows determining the structure of the plant. To this end, each shrub of rockrose was placed  
188 within a 1.45 m high, 0.9 m long and 0.9 m wide metallic frame spatially divided into 252 small  
189 cubes with sides of 15 cm. The position of each cube was indexed following its 3D (x, y, z)  
190 position. All the vegetation contained in these cubes was cut and oven dried at 60°C for 48  
191 hours. Finally, for each cube, the vegetation elements were sorted according to the six size  
192 classes (leaves, dead twigs with 0-2 mm diameter, live twigs with 0-2 mm, 2-4 mm, 4-6 mm  
193 and 6-25 mm diameters, respectively) and weighed. Thus, both live and dead fuel particles were  
194 considered. Unfortunately, this process is destructive and the characterized samples could not  
195 be used for the combustion study.

## 196 2.2. Flammability experiments

197 A series of 28 fire tests was conducted with unmodified shrubs of rockrose. The plants  
198 were harvested within the same vegetation plot that the ones used in the characterization study  
199 described above during several seasons (spring, summer and autumn). Shrubs were cut at their  
200 base and stored carefully in a room in order to preserve as well as possible their original  
201 structure. Their dimensions and weight are provided in Table 2. The average height of the shrub  
202 samples,  $h_{shrub}$  was  $1.25 \pm 0.12$  m. The average crown height and diameter were  $0.3 \pm 0.1$  m  
203 and  $0.7 \pm 0.1$  m, respectively. The overall mass of the shrubs was  $1.95 \pm 0.47$  kg on wet basis.  
204 The initial foliar moisture content (MC) of the fresh sampled shrubs was greater than 100% of  
205 the dry weight. Preliminary tests exhibited that, after ignition, the sustained combustion of  
206 shrubs with MC greater than 25% failed and their crown was not fully consumed. Furthermore,  
207 Terrei et al. [21] indicated that fire spread simulation using WFDS, at the scale of a branch, was  
208 possible if the fuel moisture content remained lower than 25%. The present study, combining  
209 experimental and numerical investigations, was thus restricted to shrubs with low MC  
210 representative of severe drought conditions [25] leading to high fire risk. The plants were air-  
211 dried during at least 48 hours in a room with an ambient air temperature of about 25°C and a  
212 relative air humidity of about 50 %. This conditioning process resulted in a foliar MC in the  
213 range of 4-18%, suitable for the combustion of the full shrub crown. About 10 g sub-samples  
214 of twigs < 2 mm in diameter with their leaves were taken from each shrub sample to determine  
215 their MC at the time of burning. These sub-samples were oven-dried at 60°C for 48 h and  
216 weighted.

217 A large-scale calorimeter was used to assess the flammability of full-scale shrubs of  
218 rockrose. Combustion took place under a 3 m × 3 m hood with a  $1 \text{ m}^3 \cdot \text{s}^{-1}$  flow rate extraction



219 system that handled the combustion products. With this device, the HRR during the combustion  
 220 of vegetation samples can be measured from oxygen consumption. The details of the technique  
 221 are provided in the next section and a layout of the experimental setup is provided in Fig. 1.  
 222 The shrubs with a structure kept almost intact compared to field conditions were mounted on a  
 223 cylindrical sample holder located on a 3 g precision load cell with full-scale capacity of 15 kg.  
 224 The balance has a voltage output for external recording of the biomass loss versus time during  
 225 thermal degradation. The measurements sampling rate was 1 Hz. A moving average method  
 226 over a 5 s-period, was used to smooth the mass recordings and estimate the mass loss rate  
 227 (MLR). Four 0.5 m × 0.5 m radiant panels were used to preheat and ignite the vegetation  
 228 samples. In order to maximize the radiation impinging on the shrub samples, two sets of two  
 229 radiant panels were used in a corner configuration in order to concentrate the emitted heat flux.  
 230 The shrub samples were positioned 2 centimeters from the radiant panels in order to avoid direct  
 231 contact which could led to instantaneous ignition of the leaves located in this region. The  
 232 maximum temperature of the radiant panels was 520°C, leading to a radiant heat flux of 20  
 233 kW.m<sup>-2</sup> impinging the nearest leaves and twigs of the shrub. Despite a lesser thermal exposure,  
 234 the electrical heaters were preferred over propane fed radiant panels, because of their fluctuating  
 235 properties. Indeed these burners induce a bias difficult to compensate during the HRR  
 236 measurement of burning shrubs. The radiant panels were left on throughout the whole  
 237 experiment to allow the shrub sample to be preheated. No pilot flame or spark igniter were used  
 238 and combustion was initiated by auto ignition. Video recordings were applied to monitor the  
 239 fire growth across the shrub. Unfortunately, flame from burning shrubs was frequently in  
 240 contact with the extraction hood, and no useful information could be obtained from the  
 241 measurement of the flame height. The metrics retained for the characterization of each  
 242 flammability component is provided in Table 1 and compared to previous literature studies. The  
 243 time to ignition (TTI) and flame duration (FD) were recorded for each fire test to measure  
 244 ignitability and sustainability, respectively. Consumability was evaluated from the fuel  
 245 consumption ratio (FCR) at both the particle level,  $\eta_k$ , and in total,  $\eta$ , defined respectively by  
 246 the following equations:

$$247 \quad \eta_k = 1 - \frac{m_{k,dry}^r}{m_{k,dry}} \quad (1)$$

$$248 \quad \eta = 1 - \frac{m_{dry}^r}{m_{dry}} \quad (2)$$

249 where  $m_{k,dry}$  and  $m_{k,dry}^r$  represent respectively the initial and residual masses of the  $k$ -class of  
 250 particles on dry basis.  $m_{dry}$  and  $m_{dry}^r$  are the initial and residual masses of the shrub,  
 251 respectively, on dry basis. In order to assess  $m_{k,dry}^r$  as a fine indicator of consumability the  
 252 vegetation characterization method (described in the previous section) was performed on burnt  
 253 samples. The assessment of the variable characterizing the last flammability component  
 254 (combustibility) is described in the next section.

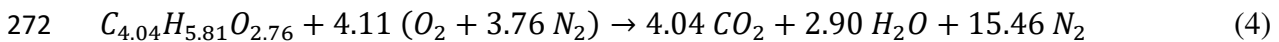
### 255 2.3. Heat release rate measurements

256 The 1 MW Large Scale Heat Release apparatus (LSHR) used to assess HRR was  
 257 manufactured and calibrated by Fire Testing Technology Limited (FTT). Probes for gas  
 258 sampling and exhaust flow rate measurement, along with laser smoke measurement, are  
 259 contained in a 0.4 m inner diameter duct insert. The measurement of the HRR is crucial for  
 260 understanding the combustion processes and assessing the flammability of materials, more  
 261 particularly for the study of full-scale plants with complex structure. The combustibility of the  
 262 samples was assessed using quantities derived from the HRR time history, namely the growth  
 263 rate and peak HRR. The growth rate was used because during the early period of the fire tests  
 264 the experimental data supported that the fires grow according to a square law, like most flaming  
 265 fires [89, 90]:

$$266 \quad HRR = \alpha t^2 \quad (3)$$

267 where  $\alpha$  and  $t$  are the fire growth parameter ( $\text{kW}\cdot\text{s}^{-2}$ ) and the time from ignition ( $\text{s}$ ), respectively.

268 As for many natural fuels, the combustion of shrub of rockrose can be represented by a  
 269 reaction of the complete combustion of lignocellulosic materials. As the experiments were  
 270 conducted under well-ventilated conditions, a stoichiometric reaction can be assumed for the  
 271 combustion of shrub of rockrose:



273 The HRR is estimated from oxygen consumption [91, 92] assuming a constant amount  
 274 of energy released per unit mass of oxygen consumed,  $E$ :

$$275 \quad HRR = E(\dot{n}_{O_2}^\circ - \dot{n}_{O_2})W_{O_2} \quad (5)$$

276 where  $W_{O_2}$  is the molecular weight of oxygen,  $\dot{n}_{O_2}^\circ$  and  $\dot{n}_{O_2}$  are the molar flow rates of  $O_2$  in  
 277 incoming air and in the exhaust duct, respectively. A more accurate estimation than the standard

278 value of the energy constant (based on average of many fuels) was determined from the fuel  
 279 ultimate analysis and low heat of combustion resulting in a value of  $E = 14.32 \text{ MJ/kg}$  of  $O_2$  for  
 280 natural fuels.

281 In order to assess the HRR, the primary measurements are the oxygen and carbon  
 282 dioxide concentrations and the exhaust flow rate. The LSHR is an open combustion system in  
 283 which the incoming air is assumed to be a mixture composed of oxygen (20.95%), carbon  
 284 dioxide, water vapour and nitrogen. During fire tests, the exhaust gases were sampled within  
 285 the duct insert at a flow rate of about  $3.5 \text{ L.min}^{-1}$ . Gas measurements were performed using  
 286  $O_2/CO_2$  analysers developed specifically for FTT calorimeters, incorporating an enhanced  
 287 Servomex 4100 featuring a high stability temperature controlled paramagnetic oxygen sensor  
 288 with flow control and by-pass for fast response time. The response time of the measurements  
 289 of the oxygen and carbon dioxide concentrations were 11 and 8 s, respectively. Water vapour  
 290 was removed from the sample gas before analysis of gas concentrations . A two-step drying  
 291 process was achieved by passing the gas sample consecutively through a cold trap and drying  
 292 column containing desiccant agent (Drierite). The exhaust flow rate was estimated using bi-  
 293 directional probe and thermocouple measurement. Accuracy was improved by the use of a  
 294 differential pressure transducer adapted to the range of flow rates.

295 The calculations of the HRR and associated parameters were automatically performed  
 296 using gas concentrations ( $O_2$  depletion and  $CO_2$  correction), exhaust flow rate and analysers  
 297 response times, based on the three following relations [91, 92]:

$$298 \quad HRR = \frac{E\rho_0 W_{O_2}}{W_{air}} (1 - X_{H_2O}^\circ) X_{O_2}^\circ \dot{V}_{s,298} \left[ \frac{\phi}{(1-\phi) + \alpha\phi} \right] \quad (6)$$

$$299 \quad \dot{V}_{s,298} = 22.4A \frac{k_t}{k_p} \sqrt{\frac{\Delta P}{T_S}} \quad (7)$$

$$300 \quad \phi = \frac{X_{O_2}^\circ (1 - X_{CO_2}) - X_{O_2} (1 - X_{CO_2}^\circ)}{X_{O_2}^\circ (1 - X_{CO_2} - X_{O_2})} \quad (8)$$

301 where  $X_i^\circ$  and  $X_i$  denotes the measured mole fraction of species  $i$  in the incoming air and  
 302 exhaust gases, respectively,  $\rho_0$  is the density of dry air at 298 K and 1 atm.,  $W_{O_2}$  and  $W_{air}$  are  
 303 the molecular weight of  $O_2$  and air, respectively,  $A$  is the cross sectional area of the duct,  $k_t$  is a  
 304 constant determined via a propane burner calibration,  $k_p=1.108$  for a bi-directional probe,  $\Delta P$

305 is the pressure drop across the bi-directional probe and  $T_s$  is the gas temperature in the duct.  
306  $\dot{V}_{s,298}$  and  $\phi$  are the standard flow rate in the exhaust duct measured in the duct insert and the  
307 expansion factor for the fraction of the air that was depleted of its oxygen, respectively.

#### 308 2.4.Data analysis

309 In order to highlight the main trends observed through the flammability and shrub  
310 variables, relationships were sought using simple linear regression (least square fitting). The  
311 equation of the linear fits and 95% confidence intervals are provided (determination coefficient  
312 and p-value are also given). Analyses were performed using R software (ver. 4.3.2, R Project  
313 for Statistical Computing).

314 Principal Component Analysis (PCA) was performed to investigate the clusters from  
315 the various flammability components and related variables, particularly among combustibility  
316 and consumability for which different regimes were observed. The previously defined  
317 component metrics were used as input parameters for the statistical analysis of global  
318 flammability. Analyses were performed using Minitab software (ver. 17.1.0, Minitab LLC).

#### 319 2.5.Numerical study

320 The Wildland-urban interface Fire Dynamics Simulator (WFDS, ver. 6.0.0) is a physical  
321 model developed by the U.S. Forest Service. It is an extension of the National Institute of  
322 Standards and Technology's structural Fire Dynamics Simulator (FDS) to forest fuels. The  
323 model is based on coupled equations governing heat and mass transfers between solid and gas  
324 phases. Large-Eddy Simulation (LES) numerical method is used to solve the conservation  
325 equations of momentum, mass and energy in the gas phase. Full details of the modeling  
326 approach are provided in [79, 80]. For the present study, the gas phase model was left  
327 untouched, the radiative fraction was estimated to be 27%, from the methodology proposed in  
328 [93]. As far as the solid phase is concerned, the thermal degradation models for the desiccation,  
329 pyrolysis and char oxidation processes are based on Arrhenius laws [79, 80]. In the condensed  
330 phase model, the bulk density  $\rho_{b,k}$  and specific heat  $c_{p,k}$  for each particle class have  
331 contributions from dry fuel, moisture content, char and ash. The solid phase equations for a  $k$ -  
332 class of particles, considered as thermally thin, are given by:

$$333 \frac{d\rho_{bk}}{dt} = -R_{k,H_2O} - (1 - \chi_{char})R_{k,pyr} - (1 - \chi_{ash})R_{k,char} \quad (9)$$

334 where  $\chi_{char} = 0.27$  is the mass fraction of dry vegetation converted to char and  $\chi_{ash} = 0.13$   
 335 represents the fraction of char converted to ash. The Arrhenius rate equations for drying,  
 336 pyrolysis, and char oxidation are

$$337 \quad R_{k,H_2O} = \rho_{bk,H_2O} A_{H_2O} T_k^{-\frac{1}{2}} e^{-\frac{E_{H_2O}}{T_k}} \quad (10)$$

$$338 \quad R_{k,pyr} = \rho_{bk,dry} A_{pyr} e^{-\frac{E_{pyr}}{T_k}} \quad (11)$$

$$339 \quad R_{k,char} = \frac{A_{char}}{\nu_{O_2,char}} \rho_g Y_{O_2} \sigma_k \beta_k e^{-\frac{E_{char}}{T_k}} (1 + \beta_{char} \sqrt{Re_k}) \quad (12)$$

340 where the values of the kinetic constants for drying, pyrolysis and char oxidation are  $A_{H_2O} =$   
 341  $600000 \text{ K}^{\frac{1}{2}} \cdot \text{s}^{-1}$ ,  $A_{pyr} = 39929 \text{ K}^{\frac{1}{2}} \cdot \text{s}^{-1}$  and  $A_{char} = 193.5 \text{ K}^{\frac{1}{2}} \cdot \text{s}^{-1}$ , respectively. The  
 342 corresponding activation energies are  $E_{H_2O} = 6262 \text{ K}$ ,  $E_{pyr} = 7389 \text{ K}$  and  $E_{char} = 8191 \text{ K}$ ,  
 343 respectively. The value of these parameters was optimized (varied at maximum of 10%  
 344 compared to previous study on pine needle beds [79]) in order to best fit the HHR curve for  
 345 shrub of rockrose.  $Re_k$  represents the Reynolds number,  $Re_k = \frac{2\rho_g |u| r_k}{\mu}$  with  $r_k = \frac{2}{\sigma_k}$ ,  $\sigma_k$  and  
 346  $\beta_k$  are the surface to volume ratio and compactness of the  $k$ -class of particles, respectively.

$$347 \quad \rho_{bk} c_{pk} \frac{dT_k}{dt} = -\Delta h_{vap} R_{k,H_2O} - \Delta h_{pyr} R_{k,pyr} - \alpha_{char} \Delta h_{char} R_{k,char} + Q_k \quad (13)$$

348 with

$$349 \quad Q_k = -\langle \dot{q}_{c,k}''' \rangle_{V_b} - \langle \nabla \cdot \dot{q}_{r,k}'' \rangle_{V_b} \quad (14)$$

350 where  $T_k$  is the temperature of the  $k$ -class of particles. The first three terms of the right-hand-  
 351 side of eq. (13) represent endothermic drying, endothermic pyrolysis and exothermic char  
 352 oxidation, respectively. The non-dimensional weighting parameters,  $\alpha_{char}$ , is the fraction of  
 353 the heat generated by the char oxidation which is absorbed by the solid fuel element and is  
 354 empirically set to 0.5 [76]. The resulting fraction of the heat transferred to the gas phase is thus  
 355  $(1 - \alpha_{char})$ . The heats of reaction for evaporation, pyrolysis and char oxidation are  $\Delta h_{vap} =$   
 356  $2259 \text{ kJ} \cdot \text{kg}^{-1}$ ,  $\Delta h_{pyr} = 418 \text{ kJ} \cdot \text{kg}^{-1}$  and  $\Delta h_{char} = -32740 \text{ kJ} \cdot \text{kg}^{-1}$ , respectively. The terms in the

357 right hand side of eq. (14) are the fuel element bulk contributions of convective and radiative  
358 heat transfer, respectively.

359

### 360 **3. Results and discussion**

#### 361 **3.1. Vegetation characterization**

362 A detailed characterization of 3 shrubs of rockrose was firstly performed in autumn  
363 paying a particular attention to the fuel elements composing it. The particles were divided into  
364 the following classes: leaves, 0-2 mm, 2-4 mm, 4-6 mm and 6-25 mm diameter twigs. Their  
365 surface area-to-volume ratio ( $\sigma$ ) was 2081, 1733, 1000, 666 and 400  $\text{m}^{-1}$ , respectively. The  
366 density ( $\rho$ ) of leaves and twigs was 478 and 961  $\text{kg}\cdot\text{m}^{-3}$ , respectively. The following data are  
367 presented on dry basis as a function of non-dimensional height  $z^* = \frac{z}{h_{shrub}}$ , where  $z$  and  $h_{shrub}$   
368 are the sampling height and shrub height, respectively. The mass distribution,  $\zeta_{k,dry}(z^*)$  and  
369 mass fraction,  $\gamma_{k,dry}(z^*)$ , of a  $k$ -class of particles, were calculated as follows:

$$370 \zeta_{k,dry}(z^*) = \frac{m_{k,dry}(z^*)}{\sum_{z^*} m_{k,dry}(z^*)} \quad (15)$$

$$371 \gamma_{k,dry}(z^*) = \frac{m_{k,dry}(z^*)}{\sum_k m_{k,dry}(z^*)} \quad (16)$$

372 where  $m_{k,dry}$  represents the mass of the  $k$ -class of particles on dry basis.

373 The mass distribution (Fig. 2.a) shows how particles of a  $k$ -class are distributed within  
374 the shrub. The thin particles (leaves and live twigs  $\leq 2$  mm in diameter) are mainly located for  
375  $z^*$  in the range of 0.77-1.00. It should be noted that they represent  $35.0 \pm 0.4$  % of the total mass  
376 of the shrub of rockrose. The Fig. 2.b displays the predominance of a class of particles over the  
377 others for a given height. As an example, large fuel elements (twigs  $> 4$  mm in diameter) are  
378 predominant for  $z^*$  in the range of 0.00-0.46. The analysis of these results allows the  
379 delimitation of three zones: the crown composed of thin particles ( $z^*$  greater than 0.77); the base  
380 composed of large particles ( $z^*$  lower than 0.46); in between the intermediate zone composed  
381 of live and dead twigs (mainly twigs in the range of 2 - 6 mm diameter).

382 The mass proportion of the different size classes of particles,  $\Gamma_{k,dry}$ , was also estimated:

$$383 \Gamma_{k,dry} = \frac{m_{k,dry}}{\sum_k m_{k,dry}} \quad (17)$$

384 Measurements show a similar distribution of particles for the 3 samples. The shrub were  
385 composed of  $22.1 \pm 0.8$  % of leaves,  $26.0 \pm 2.1$  % of twigs  $\leq 2$  mm in diameter,  $18.3 \pm 0.9$  %  
386 of twigs with diameter in the range of 2 - 4 mm,  $17.0 \pm 1.6$  % of twigs with diameter in the  
387 range of 4 - 6 mm and  $17.0 \pm 4.0$  % of twigs  $> 6$  mm in diameter. This pre-fire analysis based  
388 on size class suggests that about 48.1 % of the fuel elements are prone to burn easily (particle  
389 thickness lower than 2 mm), 18 % could burn ( $2 \text{ mm} < \text{diameter} \leq 4 \text{ mm}$ ) and 34 % might not  
390 burn ( $> 4$  mm in diameter).

391 Based on these experimental measurements, the distribution of the bulk density within  
392 the shrub was established for each particle size class (Table 3). Bulk density refers to the dry  
393 mass of fuel elements (leaves and different diameter twigs) per unit volume. These data will be  
394 used as input parameters for the numerical study. In the next section the influence of these  
395 characteristics on the overall plant flammability is investigated.

### 396 3.2. Four components of flammability

397 The whole burning process of a shrub of rockrose, from ignition to flameout, is  
398 displayed in Fig. 3. The several phases during which the four flammability components were  
399 measured through previously defined metrics, are also provided. When being exposed to  
400 external radiant heat flux, vegetation temperature increases, desiccation and thermal  
401 degradation occur. Combustible gases are released and mixed with ambient air. A small flame,  
402 generated by the ignition of this gas mixture by hot glowing particles, quickly engulfed the fuel  
403 elements located nearby. Leaves were observed to be the class of particles that first ignites due  
404 to their high surface-to-volume ratio. Ignition was always located at the edge of the crown  
405 (location where external heat flux is maximum and leaves are the most abundant) but due to the  
406 corner configuration of the radiant panels, double ignition could occurred in some rare cases.  
407 The fire spread always forward across the crown (leaves and small diameter twigs) and  
408 sometimes downward across the intermediate zone (burning greater diameter twigs) depending  
409 on the fire heat released. A short ( $23 \pm 10$  s) quasi-steady burning period was observed followed  
410 by a rapid decay of HRR burnt out. The shrub combustion was incomplete, with char residues  
411 and unburnt material located at both the base and intermediate zone of the shrub. Despite the  
412 care taken to select plants to be harvested, small discrepancies at particle level (twigs with  
413 leaves protruding out of the crown, discontinuity within the crown, trapezoidal instead of  
414 spherical crown shape...) yielded to different fire behaviors that will be examined through the  
415 flammability components in the following sections.

416

### 3.2.1. Ignitability

417 Ignitability was studied for an external radiant heat flux of  $20 \text{ kW}\cdot\text{m}^{-2}$  as would happen  
418 when a flame front, driven by buoyancy effects, approaches vegetation [94]. The difference of  
419 importance between the present work and previous studies conducted on full shrubs is that, in  
420 the latter, ignition was piloted and performed using a flame at the base of the plant [10, 18, 30-  
421 43] instead of auto-ignition. The air drying process at room temperature, resulted in shrub foliar  
422 MC in the range of 4-18% on dry basis depending on the initial MC of the samples and drying  
423 time. The MC of the particles of other size classes was higher than the one of the leaves. For  
424 instance, the corresponding MC for the smaller twigs (diameter  $< 2 \text{ mm}$ ) was in the range of  
425 10-45 %. The larger the fuel element diameter, the higher the MC. Even after drying, the shrubs  
426 with foliar MC greater than 20% did not burn entirely once ignited and these fire tests were not  
427 considered for the flammability study. Even under these low foliar MC conditions, ignitability  
428 was difficult to assess using external radiant heat flux only as ignitor. Other works also observed  
429 flame extinguishment before much of the plant burned and thus used a pilot flame as ignition  
430 source [21] often combined with wind [52, 53] in order to observe sustained combustion of the  
431 vegetation samples. The TTI dependence on the MC of the leaves is plotted on Fig. 4 for shrubs  
432 harvested in autumn and summer. Despite their scattering ( $R^2=0.585$ ), the data exhibit an  
433 increase of the TTI with increasing MC. The reasons of this scattering can be found in the  
434 impossibility to have by nature strictly identical test specimen when working with unmodified  
435 plants. The slight changes existing between the structure (position of the leaves within the  
436 crown) of the different shrub samples was observed to influence ignitability. The increase of  
437 MC decreases the shrub ignitability by requiring more energy for preheating of the fuel and for  
438 water evaporation, in accordance with literature [24, 43, 95, 96]. Previous flammability tests  
439 [14] conducted on various Mediterranean natural fuels, using ignition apparatus, also found a  
440 linear relationship between ignitability and moisture content. Nevertheless, the bulk density of  
441 the vegetation samples considered in these small-scale fire tests tends to be overestimated  
442 compared to the one of full plants. In another work [23], the authors conducted experimental  
443 study submitting live leaves of various species with MC in the range of 35-200% to very high  
444 heat fluxes from a flame ( $80\text{-}140 \text{ kW}/\text{m}^2$ ). They concluded that both TTI and ignition  
445 temperature showed no dependence on foliar MC. Nevertheless, fire tests carried out at high  
446 external radiant heat flux ( $\geq 50 \text{ kW}/\text{m}^2$ ) or very high mixed convective-radiative heat flux (pilot  
447 flame) [11, 21, 52, 53] may tend to mask the possible differences between samples at different  
448 foliar MC levels because too rapid ignition occurs [9, 37]. Ignitability was already observed to



449 be highly dependent on the type of ignition source and scale [11, 96]. Babrauskas [97] also  
450 discussed the effects of the variety of external heat sources on ignition of vegetation.  
451 Unfortunately, the test procedure and particularly the ignition method for plants parts and  
452 furthermore for full scale shrubs is not standardized yet. As a result, a wide range of radiation  
453 levels (15-50 kW/m<sup>2</sup>) can be found in the literature. Furthermore, many studies provide the  
454 temperature of the radiant heater instead of heat flux and the comparison is not easy. Martin et  
455 al. [5] first suggested that ignitability should be described in terms of time to ignition per rate  
456 of energy per unit area in order to take into account the heat flux impinging on the vegetation  
457 sample.

### 458 3.2.2. *Combustibility*

459 Combustibility was defined in terms of both fire growth and peak HRR. A subset of the  
460 data, excluding samples of shrub of rockrose harvested in summer, was considered for the study  
461 of combustibility, sustainability and consumability due to large difference in crown structure  
462 compared to other seasons. Indeed, the persistence of flowers and seeds on the early summer  
463 shrubs altered significantly their combustion dynamics and resulting global flammability. Once  
464 ignited, burning seeds falling on the ground were observed to make a major contribution to the  
465 mass loss but a very limited contribution to the heat release. Furthermore, these incandescent  
466 fuel elements are prone to generate secondary ignition points within the crown, influencing the  
467 overall combustion of the shrub. On the other hand, up to the ignition of the leaves, the behavior  
468 of the shrubs containing seeds was not influenced by their presence. For this reason, the data  
469 on the TTI of the summer shrubs were kept when ignitability was studied. In whole plant fire  
470 tests, the rates of fire growth and heat released are related to the rate of spread of the fire across  
471 the sample and this metrics could also be used to study combustibility [5]. The data analysis  
472 distinguished three main types of combustibility according to the growth rate and peak HRR.  
473 Curves of HRR versus time corresponding to low ( $\alpha = 0.10 \text{ kW}\cdot\text{s}^{-2}$ ), medium ( $\alpha = 0.22 \text{ kW}\cdot\text{s}^{-2}$ )  
474 and high combustibility ( $\alpha = 0.52 \text{ kW}\cdot\text{s}^{-2}$ ) are plotted in Fig. 5. The corresponding fires images,  
475 taken 30 s after ignition, are provided in Fig. 6. It should be noticed that the values of the fire  
476 growth parameter  $\alpha$  obtained for the plant composed of fine particles do not match the standard  
477 range (NFPA, 92B [98]) of *t*-squared fires typical of fuels encountered in fire safety for  
478 buildings (paper, cardboard, foam...) due to the high porosity and low mass of the shrub crown,  
479 resulting in much lower flame duration. In the present study, for  $\alpha$  values lower than  $0.2 \text{ kW}\cdot\text{s}^{-2}$   
480 <sup>2</sup>, the fire growth rate was considered as slow (whereas it corresponds to ultrafast fire growth  
481 for building materials). The fire spread across the crown was slow and flames were observed to

482 travel from a branch supporting leaves to another one, resulting in low average peak HRR of  
483  $100 \pm 5$  kW. Consequently, the resulting combustibility was defined as low. Medium fire  
484 growth rate and moderate combustibility were observed for  $\alpha$  values in the range of 0.2-0.4  
485  $\text{kW}\cdot\text{s}^{-2}$ . The fire spread horizontally from the ignition zone towards the opposite edge of the  
486 crown with average peak HRR of  $188 \pm 27$  kW. Finally, for  $\alpha$  values higher than  $0.4 \text{ kW}\cdot\text{s}^{-2}$ ,  
487 the fire spread horizontally at a fast rate throughout the entire thin classes of particles located  
488 within the crown and then spread vertically downwards through the thicker classes thanks to a  
489 higher heat feedback towards the base of the shrub. Combustibility was high and the fire  
490 consumed larger diameter particles with high heat release rate (average peak HRR of  $257 \pm 63$   
491 kW). It should be pointed out that the linear relationship between peak HRR and peak MLR  
492 exhibits a regression value of the heat of combustion of  $13.9 \text{ MJ}\cdot\text{kg}^{-1}$  ( $R^2 = 0.911$ ).

493 The fire growth parameter was found to strongly depend on the quantity of foliar  
494 biomass above the ignition location. The greater the amount of fuel, the greater the fire growth  
495 parameter. When ignition occurs in the region located between the bottom and the middle of  
496 the crown, the convective heating of the fuel elements by flame impingement along the full  
497 crown height cause a fast fire growth rate that maximize the heat transfer mechanisms. In the  
498 following, ignition that occurred in this region will be called as “favorable” whereas ignition  
499 located above it will be called as “unfavorable”.

500 In the present study, the combustibility was assessed using two characteristics of the  
501 HRR, namely its growth rate and peak value. Previous studies [8, 9, 11-13, 18, 19, 21, 40, 46,  
502 99] used flame height or maximum air temperature above the sample (which depends on the  
503 placement of the thermocouples) that are not relevant descriptors. Indeed, combustibility was  
504 defined as how well or rapidly a fuel burns [4]. If HRR cannot be evaluated, the metrics used  
505 should be rather based on a rate such as the rate of fire spread across the sample, the rate of  
506 temperature increase of the fuel material or better the MLR. Indeed, the MLR can also be used  
507 as metrics for combustibility (and not consumability [9, 11, 21]), since it is related to HRR by  
508 a constant (effective heat of combustion). As already pointed out [9], the standardization among  
509 test procedures to assess the flammability components is necessary.

### 510 3.2.3. Sustainability

511 After growth, the fire reached a short quasi-steady burning stage. The data exhibit that  
512 flame duration is related to combustibility and decreases with increasing fire growth parameter  
513 and peak HRR (Fig. 7). Data also shows scattering for the reasons previously given for the

514 ignitability study. Flame duration (FD) in the range of 80 - 120 s were observed for low peak  
515 HRR ( $\leq 150$  kW), while shorter FD (around 40 s) were obtained for high peak HRR ( $\geq 210$   
516 kW). Sustainability was also found to depend on the amount of fuel elements present above the  
517 ignition location. Indeed, under favorable ignition conditions, the flame quickly engulfed most  
518 of the shrub crown resulting in a short FD and high combustibility (high fire growth parameter  
519 and peak HRR). Conversely, unfavorable ignitions resulted in slow horizontal propagation. In  
520 this case, heat transfers to the unburnt particles are mainly dominated by radiation since the  
521 flame did not impinge these fuel elements. The fire could stop because of fuel discontinuity  
522 which was too large to result in significant convective heat transfer. Such regime of fire spread  
523 exhibited slow rate of spread, long FD and low peak HRR. Authors generally agree on the  
524 definition of sustainability that is easy to estimate from direct visual observations or from  
525 measurements of various quantities (temperature above threshold). Nevertheless, the wide  
526 variety of scales and experimental procedures render the comparison difficult. Indeed, FD is  
527 highly dependent on the mass of the fuel, presence of wind but also on ignition characteristics  
528 and heat release to sustain combustion of the plant.

#### 529 3.2.4. Consumability

530 In order to provide an detailed representation of the particle size classes involved in the  
531 combustion process, the fuel consumption at particle level was estimated from the residual mass  
532 fraction. It is defined as:

$$533 \tau_{k,dry}(z^*) = \frac{m_{k,dry}^r(z^*)}{m_{k,dry}(z^*)} \quad (18)$$

534 where  $m_{k,dry}^r$  represents the mass of remaining fuel of the  $k$ -class of particles on dry basis. Pre-  
535 fire (3 samples) and post-fire (test 15) comparison of the distribution along the non-dimensional  
536 height ( $z^*$ ) of mass fractions is provided in Fig. 8 for the different classes of particles. Since  
537 these characterization measurements consist of destructive sampling, the shrubs to be burnt  
538 could unfortunately not be characterized using this method. The use of LIDAR-based technique  
539 should be a suitable alternative for the estimation of fuel element distribution within the  
540 vegetation [100]. In this particular fire test (Peak HRR of 264 kW), the total fuel consumption  
541 ratio was 42%. For most of the fire tests, the crown ( $z^* > 0.77$ ) was fully consumed and the  
542 intermediate zone was partially consumed ( $0.6 > z^* > 0.77$ ). Compared to initial mass fractions,  
543 the lower values measured in the burnt shrub, indicates that all the foliage and part of the

544 particles lower than 6 mm in diameter were burnt while the 6 - 25 mm size class did not undergo  
545 thermal degradation.

546 Consumability was also evaluated from the total quantity of fuel consumed by the fire  
547 tests. The effect of foliar moisture content on fuel consumption ratio (FCR) is displayed in Fig.  
548 9. The FCR holds a decreasing trend with increasing MC of the leaves in agreement with  
549 previous studies [30, 43, 47]. These results suggest that MC alters the thermal degradation  
550 processes as a fire retardant. The average mass lost for all experiments was  $0.52 \pm 0.2$  kg which  
551 is equivalent to a fuel consumption ratio of  $25 \pm 8\%$ . Observations during experiments and  
552 characterization at the particle level show that the mass was quasi exclusively consumed in the  
553 crown which is mainly composed of fine fuel elements (leaves and 0 - 2 mm diameter twigs)  
554 that represent 35% of the total dry mass of the shrub. Based on the characterization study and  
555 the FCR values obtained, the consumability can be categorized into the three basic types. A  
556 FCR below 18% indicates that the leaves were not fully consumed. The fire did not spread  
557 across the whole crown resulting in a low consumability. A medium consumability proceeds  
558 from a FCR in the range of 18 - 33%, where all the leaves and part of the 0 - 2 mm class particles  
559 in the crown were consumed. Finally, FCR greater than 33% indicates a full consumption of  
560 the crown and a part of the classes of particles in the range of 0 - 4 mm located within the  
561 intermediate zone of the shrub of rockrose. The fuel elements larger than 4 mm were partly  
562 consumed only when the peak of HRR was high enough ( $250 \pm 10$  kW). It should be noted that  
563 fire tests were carried out on conditioned shrub and the initial dry mass could not be measured  
564 but only estimated from the wet mass, MC and distribution of each particles size class. Thus,  
565 the uncertainty related to the estimation of the dry mass directly affects the calculation of the  
566 consumed mass fraction.

### 567 3.3. Characterization of different flammability regimes

568 The same variables as the one used for metrics for the components (FD, peak HRR, peak  
569 MLR, fire growth parameter and FCR) were used as input parameters of PCA, except for  
570 ignitability where ignition location variable was introduced. Indeed, the use of TTI as a variable  
571 for the analysis did not allow to distinguish group tests with similar flammability. When using  
572 ignition location instead of TTI, two fire tests from the same cluster exhibited more similar  
573 flammability regimes than two tests from different clusters. The concept of flammability is thus  
574 revisited in the present approach. A variable of great importance, linked to the random ignition  
575 location, is introduced. Indeed, working with natural shrub samples, that show discrepancies,

576 introduce supplementary difficulties compared to studies carried out at the lower scales, with  
577 more similar samples (isolated fuel elements or leafy branch). If strictly identical shrub samples  
578 were considered and ignition always occurred in the same area (which is not possible with  
579 unmodified vegetation), the TTI would have been an important factor in differentiating the  
580 flammability regimes from PCA. In the present study, the ignition location occurred in different  
581 areas according to the crown structure and significantly influenced the resulting flammability.  
582 When ignition occurs in the region located between the bottom and the middle of the crown,  
583 the convective heating of the fuel elements by flame impingement along the full crown height  
584 drastically increases the heat transfer mechanisms and causes a fast fire growth rate. PCA  
585 reveals that three principal components (PC) explain a total of 87% of the variance (Fig. 10.a).  
586 PC 1 explains 54% of the variation in the data. The fire growth parameter, peak HRR, peak  
587 MLR characterize PC1 which is therefore representative of both combustibility and  
588 sustainability. Ignition location and FCR characterize PC 2 (19% of the variance) and PC3 (14%  
589 of the variance, not shown in Fig. 10.a), respectively. Sustainability and combustibility are  
590 negatively correlated (opposed). Indeed, the shrub samples exhibiting high combustibility  
591 during fire tests typically sustained flame for a shorter duration. The projection of the  
592 combustion experiments on the factorial map in the plane (PC 1, PC 2) revealed four clusters  
593 of fire tests (Fig. 10.b). Color and black markers refer to single experiment and barycenter of  
594 the corresponding flammability group, respectively. Four types of flammability were identified  
595 for this plant species:

- 596 • The first group (circles) corresponds to fire tests with low flammability, low  
597 combustibility ( $\alpha$  values lower than  $0.2 \text{ kW}\cdot\text{s}^{-2}$  and a low peak HRR of  $83.9 \pm 20 \text{ kW}$ ),  
598 high sustainability (very long FD of  $100 \pm 14 \text{ s}$ ) and low consumability (weak FCR of  
599  $18.9 \pm 3.0\%$ ). Combustion solely involves leaves and 0-2 mm diameter twigs.
- 600 • The second group (squares) is the group of medium flammability with medium  
601 combustibility ( $\alpha$  values in the range of  $0.2 - 0.4 \text{ kW}\cdot\text{s}^{-2}$ , medium peak HRR of  $188 \pm$   
602  $27 \text{ kW}$ ), high sustainability (long FD of  $77 \pm 10 \text{ s}$ ) and moderate consumability (FCR  
603 of  $23 \pm 5\%$ ). Combustion involves leaves and particles size class up to 4 mm in diameter.
- 604 • The third group (diamonds) is characterized by high combustibility ( $\alpha$  values  
605 greater than  $0.4 \text{ kW}\cdot\text{s}^{-2}$ , high peak HRR of  $228 \pm 15 \text{ kW}$ ), low sustainability (short FD  
606 of  $44 \pm 9 \text{ s}$ ) and moderate consumability (moderate FCR ( $25 \pm 6\%$ )). This high  
607 flammability with low sustainability group involves the same classes of particles as the  
608 medium flammability.

609 • The last group (triangles) exhibits high combustibility ( $\alpha$  values greater than 0.4  
610  $\text{kW}\cdot\text{s}^{-2}$ , very high peak HRR of  $384 \pm 99 \text{ kW}$ ), high sustainability (long FD of  $70 \pm 14$   
611 s) and high consumability (high FCR of  $32 \pm 4\%$ ). This high flammability with high  
612 sustainability (or hot flammability under the evolutionary concept define by Pausas  
613 [17]) includes consumption of particles with diameter greater than 4 mm.

614 Four regimes of flammability were defined for shrubs of rockrose within the same range of  
615 size and shape. Despite a similar shape of the shrub samples, small changes in their structure  
616 can significantly affect how they are heated by both convection and radiation and subsequently  
617 their flammability as pointed out by [9, 47, 66-70, 101]. The differences between the different  
618 flammability regimes are mainly explained by the ignition position, the proportion of the thin  
619 fuel elements within the crown and the radiant exposure time. Unfavorable ignition causes low  
620 or medium flammability, while favorable ignition results in high flammability. The structure of  
621 the vegetation explains the discrepancies between low and medium flammability where  
622 estimated foliar bulk density were  $2.35 \pm 0.64 \text{ kg}\cdot\text{m}^{-3}$  and  $4.65 \pm 0.72 \text{ kg}\cdot\text{m}^{-3}$ , respectively. A  
623 low bulk density tends to decrease the potential heat release and related fire spread across the  
624 shrub crown. In the case of high flammability, the difference between low and high  
625 sustainability regimes is mainly caused by radiant exposure time. For the high flammability  
626 with high sustainability regime, long exposure time ( $>400 \text{ s}$ ) allowed relatively more preheating  
627 and desiccation of the plant. The MC of the overall particle size classes was thus considerably  
628 reduced when ignition occurs, resulting in high consumability. Indeed, the thermal degradation  
629 also occurred for twigs greater than 4 mm in diameter. For shorter exposure time (high  
630 flammability with low sustainability), these large diameter twigs did not receive enough heat to  
631 achieve desiccation and reach ignition.

### 632 3.4. Simulation results

633 The characterization of the shrub detailed in the previous section (distribution of bulk  
634 density of all fuel particle classes and their related MC) provided necessary data for the model  
635 inputs. We first used a rectangular grid to model the shrub based on this characterization.  
636 However, the cube-based mesh did not match perfectly a shrub's envelope and the crown bulk  
637 density was underestimated at the edges. A more suitable model for the geometry, composed  
638 of six superposed 0.15 m high frustums with varying radius along the height, were used instead  
639 of cubes. Each frustum encompasses 6 fuel layers corresponding to the 6 particle size classes.

640 The dry bulk density  $\rho_{bk}$  of each particle size classes at the mean height of a frustum,  $z$ , was  
641 determined from the mass measurements (Table 3) by:

$$642 \quad \rho_{bk}(z) = \frac{m_{k,dry}(z)}{V(z)} \quad (19)$$

643 where  $V(z)$  represents the volume of the frustum and  $m_{k,dry}(z)$  is the mass on dry basis of the  
644  $k$ -class of particles in the frustum. The grid resolution needed to perform the simulations was  
645 estimated from two characteristic length scales associated with two physical phenomena  
646 involved in the combustion. The first one corresponds to the extinction length,  $\delta_R$ , which  
647 represents the absorption of radiation by vegetation.  $\delta_R$  is given by:

$$648 \quad \delta_R = \frac{4}{\beta_k \sigma_k} \quad (20)$$

649 The grid size used within the shrub,  $dx_b$  must be of the order of one fifth of  $\delta_R$  [80, 102].  
650 The grid resolution  $d_x$  in the gas phase region (flame and buoyant plume) is related to the  
651 diameter of the fire,  $z_c$ , which represents the second characteristic length scale. McGrattan et  
652 al. [58] proposed the following relationship to determine  $z_c$ :

$$653 \quad z_c = \left( \frac{\dot{q}}{\rho_\infty c_p T_\infty \sqrt{g}} \right)^{\frac{2}{5}} \quad (21)$$

654 where  $\dot{q}$ ,  $\rho_\infty$ ,  $c_p$ ,  $T_\infty$  and  $g$  are the HRR, the density, specific heat and temperature of the ambient  
655 air and the gravitational acceleration, respectively. The authors suggested a ratio  $z_c/d_x$  in the  
656 range of 4 - 16. The extinction length was calculated from the numerical shrub characteristics.  
657 A value of 0.144 m was obtained for  $\delta_R$  which leads to a grid size lower than 0.029 m.  
658 Concerning the mesh size for the flow,  $z_c$  was calculated from the peaks of HRR obtained for  
659 the four flammability regimes. The minimum value of  $z_c = 0.356$  m was obtained for the low  
660 flammability fire tests with a measured average peak HRR of 100 kW. The value of  $z_c$   
661 suggested  $d_x$  in the range of 0.022-0.089 m. Based on these results, the mesh size was chosen  
662 as the minimum of  $d_x$  and  $dx_b$  (0.02 m) in both domains for the shrub and surrounding gas.  
663 The whole computational domain includes the extraction hood and the radiant panels in order  
664 to fully match the experimental conditions. A preliminary simulation was carried out in order  
665 to check the agreement between predicted and measured radiant heat flux density from the  
666 radiant panels heated at 520°C. WFDS succeeded to predict auto ignition of the shrub, but the  
667 simulated flame did not release enough heat to sustain the combustion and fire spread across

668 the shrub. Thereby, a piloted ignition was added, consisting of fuel elements kept at a  
669 temperature of 1000°C for a given time. The ignitor was set on when the predicted pyrolysis  
670 mass loss due to preheating had reached the experimental one. Its duration (15 s) was then fitted  
671 for the fire to sustain spread. As a first step to investigate the numerical burning of a shrub, the  
672 simulations performed with WFDS were conducted for the high flammability with low  
673 sustainability regime which experimental results exhibited the best reproducibility. The ignitor  
674 was set in the lower part of the crown and its volume ( $10 \times 20 \times 20 \text{ cm}^3$ ) corresponds to the size  
675 of the flame observed during the experiments at ignition. This location corresponds to a  
676 favourable ignition as mentioned in the experimental section.

677 Based on the experiments, average moisture contents were used for the different size classes  
678 of particles (Table 3). The comparison of the predicted and measured fire spread at different  
679 times is provided in Fig. 11. A  $200 \text{ kW.m}^{-3}$  iso-contour of volumetric heat release rate was  
680 retained for the visual representation of the flame that nearly corresponds to a  $500^\circ\text{C}$  iso-  
681 surface. The corresponding predicted and measured HRR and MLR over time are plotted in  
682 Fig. 12. The predicted HRR is the sum of the heat released by gas phase reactions within the  
683 flame and solid phase due to the char oxidation. The main discrepancy in the curves compared  
684 to measurements can be found in the presence of a plateau just after ignition. The reasons for  
685 this difference can be attributed to the Arrhenius law used for the formulation of the thermal  
686 degradation. The predicted peak HRR (215 kW) compares favourably to the measured one ( $226 \pm 24 \text{ kW}$ ).  
687 The predicted (and measured) mass consumed and peak MLR were 0.36 kg ( $0.58 \pm$   
688  $0.17 \text{ kg}$ ) and  $0.012 \text{ kg.s}^{-1}$  (and  $0.015 \pm 0.003 \text{ kg.s}^{-1}$ ), respectively. The prediction of the flame  
689 duration (42 s) is also in agreement with the one measured during the experiments ( $44 \pm 9 \text{ s}$ ).  
690 The faster predicted decay phase may be caused by an overestimation of the particles cooling  
691 with fresh air after the flameout. The resulting mass consumption is underestimated due to a  
692 rapid extinction of the char after the flameout. As far as FCR is concerned, the predicted value  
693 (31%) is close to measurements ( $32 \pm 8\%$ ). Despite differences during fire growth and decay  
694 phases, the model predictions are in good agreement with experimental data. The vertical  
695 distribution of the bulk density of the thin fuel elements of the shrub of rockrose ( $\rho_b <$   
696  $6 \text{ kg/m}^3$ ) is comparable to the one of another shrub species (chamise) considered in previous  
697 studies [30, 78] combining fire experiments and numerical simulation based on large eddy  
698 simulation. The thermal degradation of the fuel elements predicted in the present approach is  
699 consistent with these previous works. For a shrub of chamise, predicted (and measured) mass  
700 consumed and peak MLR were 0.49 kg ( $0.48 \pm 0.11 \text{ kg}$ ) and  $0.044 \text{ kg.s}^{-1}$  ( $0.030 \pm 0.01 \text{ kg.s}^{-1}$ ),



701 respectively. Due to the different ignition procedure (pilot flame at the base of the shrub) the  
702 resulting MLR and total mass consumed were greater for the chamise fire tests. Terrei et al.  
703 [21] also found a good agreement between WFDS predictions and measurements of both mass  
704 losses and temperatures at the scale of a branch. The present results confirm that WFDS can  
705 provide an accurate assessment flammability for a full scale plant.

706

#### 707 **4. Conclusion**

708 In the present study, experimental data was collected on the structure and flammability of  
709 individual shrubs of rockrose. The use of oxygen consumption calorimetry on full-scale plants  
710 was a substantial step forward to quantify flammability and improve the knowledge on the  
711 combustion of these natural fuels.

712 Shrubs of rockrose were characterized to obtain accurate measures of the proportion and  
713 distribution of mass for different size classes of particles from base to crown. The latter  
714 embodies thin fuel elements that were observed to play a critical role during combustion and  
715 represent the main part of the consumed biomass. The flammability of the shrubs was analyzed  
716 using some of the usual measurements. The time to ignition, used as metric for ignitability,  
717 decreases with the foliar MC. The HRR (growth rate and Peak value) and the flame duration,  
718 indicators combustibility and sustainability, respectively, were influenced by the location of the  
719 ignition within the crown. The lower the position, the higher the peak HRR and the shorter the  
720 flame duration. The FCR, metrics for consumability, increases with decreasing foliar MC. The  
721 comparison to previous experimental studies highlighted the necessity of standardization  
722 among test procedures to assess the flammability components of plants, more particularly at  
723 full scale. Finally, a statistical analysis exhibited four types of flammability depending on the  
724 ignition zone, HRR and consumed mass of thin fuel elements.

725 The shrub characterization and fire experiments carried out were used as a comparison basis  
726 for the predictions of WFDS. This study highlighted the capacity of WFDS to predict the main  
727 fire characteristics (peak HRR, flame duration and consumption rate). However, simulations  
728 results showed a plateau in the HRR after the ignition that alters the predicted fire growth. The  
729 extinction of the char smoldering phase was too fast, probably due to an overestimation of the  
730 convective cooling. An investigation on the causes of these discrepancies through more  
731 thorough investigation of the degradation laws needs to be addressed.

732 Experimental results will need to be scaled-up to field conditions and include the interaction  
733 of multiple shrubs. The large scale heat release apparatus also offers the possibility to expand  
734 the study beyond a single plant and explore the interactions among several shrubs on the fire  
735 behavior and flammability. Future works need also to take into account litter fuels at the base  
736 of the shrub that were observed to contribute significantly to shrub flammability [49].

737

738 **Acknowledgements:** The authors are grateful to David Perez-Merino of the Université de  
739 Nancy, for his valuable contribution on the WFDS simulation runs.

740

## 741 **References**

- 742 [1] W.M. Jolly, M.A. Cochrane, P.H. Freeborn, Z.A. Holden, T.J. Brown, G.J. Williamson,  
743 D.M. Bowman, Climate-induced variations in global wildfire danger from 1979 to 2013, *Nature*  
744 *Communications* 6 (2015) 7537.
- 745 [2] J. San-Miguel-Ayanz, T. Durrant, R. Boca, G. Libertà, A. Branco, D.d. Rigo, D. Ferrari, P.  
746 Maianti, T.A. Vivancos, H. Costa, F. Lana, P. Löffler<sup>5</sup>, D. Nuijten, T. Leray, Forest fires in  
747 Europe, Middle East and North Africa 2017, Publications Office of the European Union,  
748 Luxembourg, 2018.
- 749 [3] NICC, Wildland Fire Summary and Statistics Annual Report 2017, National Interagency  
750 Coordination Center, Boise, Idaho, 2017.
- 751 [4] H.E. Anderson, Forest fuel ignitibility, *Fire Technology* 6 (1970) 312-319.
- 752 [5] R. Martin, D. Gordon, M. Gutierrez, D. Lee, D. Molina, R. Schroeder, D. Sapsis, S.  
753 Stephens, M. Chambers, Assessing the flammability of domestic and wildland vegetation, in:  
754 M. Society of American Foresters: Bethesda (Ed.) Proceedings of the 12th conference on fire  
755 and forest meteorology, Jekyll Island, GA, 1994, pp. 130–137.
- 756 [6] E.H. Mak, Measuring foliar flammability with the limited oxygen method, *Forest Science*  
757 17 (1988) 253–259.
- 758 [7] M. Guijarro, C. Hernando, C. Díez, E. Martínez, J. Madrigal, C. Lampin-Cabaret, L. Blanc,  
759 P.Y. Colin, P. Pérez-Gorostiaga, J.A. Vega, Flammability of some fuel beds common in the  
760 South-European ecosystems, IV International Conference on Forest Fire Research, Coimbra,  
761 Portugal, 2002.
- 762 [8] A. Ganteaume, J. Marielle, L.-M. Corinne, C. Thomas, B. Laurent, Effects of vegetation  
763 type and fire regime on flammability of undisturbed litter in Southeastern France, *Forest*  
764 *Ecology and Management* 261 (2011) 2223-2231.
- 765 [9] R.H. White, W.C. Zipperer, Testing and classification of individual plants for fire  
766 behaviour: plant selection for the wildlandurban interface, *International Journal of Wildland*  
767 *Fire* 19 (2010) 213-227.
- 768 [10] M.P. Plucinski, W.R. Catchpole, Predicting ignition thresholds in litter layers, MODSIM  
769 2001: International Congress on Modelling and Simulation, Canberra, Australia, 2001, pp. 967–  
770 971.
- 771 [11] J. Madrigal, E. Marino, M. Guijarro, C. Hernando, C. Díez, Evaluation of the flammability  
772 of gorse (*Ulex europaeus* L.) managed by prescribed burning, *Annals of Forest Science* 69  
773 (2012) 387-397.

774 [12] V.M. Santana, R.H. Marrs, Flammability properties of British heathland and moorland  
775 vegetation: models for predicting fire ignition, *Journal of environmental management* 139  
776 (2014) 88-96.

777 [13] A.L. Behm, M.L. Duryea, A.J. Long, W.C. Zipperer, Flammability of native understory  
778 species in pine flatwood and hardwood hammock ecosystems and implications for the  
779 wildland-urban interface, *International Journal of Wildland Fire* 13 (2004) 355-365.

780 [14] A.P. Dimitrakopoulos, K.K. Papaioannou, Flammability Assessment of Mediterranean  
781 Forest Fuels, *Fire Technology* 37 (2001) 143-152.

782 [15] A. Ganteaume, M. Jappiot, C. Lampin, M. Guijarro, C. Hernando, Flammability of some  
783 ornamental species in wildland-urban interfaces in southeastern France: laboratory assessment  
784 at particle level, *Environmental management* 52 (2013) 467-480.

785 [16] D.W. Schwilk, Dimensions of plant flammability, *New Phytologist* 206 (2015) 486-488.

786 [17] J.G. Pausas, J.E. Keeley, D.W. Schwilk, Flammability as an ecological and evolutionary  
787 driver, *Journal of Ecology* 105 (2017) 289-297.

788 [18] L.D. Prior, B.P. Murphy, D.M. Bowman, Conceptualizing Ecological Flammability: An  
789 Experimental Test of Three Frameworks Using Various Types and Loads of Surface Fuels, *Fire*  
790 1 (2018) 18.

791 [19] S.H. Essaghi, M.; Yessef, M.; Dehhaoui, M.; El Amarty, F., Assessment of Flammability  
792 of Moroccan Forest Fuels: New Approach to Estimate the Flammability Index, *Forests* 8  
793 (2017).

794 [20] P. Jaureguiberry, G. Bertone, S. Díaz, Device for the standard measurement of shoot  
795 flammability in the field, *Austral Ecology* 36 (2011) 821-829.

796 [21] L. Terrei, A. Lamorlette, A. Ganteaume, Modelling the fire propagation from the fuel bed  
797 to the lower canopy of ornamental species used in wildland-urban interfaces, *International*  
798 *Journal of Wildland Fire* 28 (2019) 113-126.

799 [22] D.R. Weise, R.H. White, F.C. Beall, M. Etlinger, Use of the cone calorimeter to detect  
800 seasonal differences in selected combustion characteristics of ornamental vegetation,  
801 *International Journal of Wildland Fire* 14 (2005) 321-338.

802 [23] T.H. Fletcher, B.M. Pickett, S.G. Smith, G.S. Spittle, M.M. Woodhouse, E. Haake, D.R.  
803 Weise, Effects of moisture on ignition behavior of moist California chaparral and Utah leaves,  
804 *Combustion Science and Technology* 179 (2007) 1183-1203.

805 [24] G.M. Davies, C.J. Legg, Fuel Moisture Thresholds in the Flammability of *Calluna vulgaris*,  
806 *Fire Technology* 47 (2011) 421-436.

807 [25] S. McAllister, D.R. Weise, Effects of Season on Ignition of Live Wildland Fuels Using the  
808 Forced Ignition and Flame Spread Test Apparatus, *Combustion Science and Technology* 189  
809 (2017) 231-247.

810 [26] K.J. Simpson, B.S. Ripley, P.-A. Christin, C.M. Belcher, C.E.R. Lehmann, G.H. Thomas,  
811 C.P. Osborne, Determinants of flammability in savanna grass species, *Journal of Ecology* 104  
812 (2016) 138-148.

813 [27] D.M.J.S. Bowman, B.J. French, L.D. Prior, Have plants evolved to self-immolate?,  
814 *Frontiers in Plant Science* 5 (2014).

815 [28] B.M. Pickett, C. Isackson, R. Wunder, T.H. Fletcher, B.W. Butler, D.R. Weise,  
816 Experimental measurements during combustion of moist individual foliage samples,  
817 *International Journal of Wildland Fire* 19 (2010) 153-162.

818 [29] V. Babrauskas, Effective heat of combustion for flaming combustion of conifers, *Canadian*  
819 *Journal of Forest Research* 36 (2006) 659-663.

820 [30] A. Dahale, S. Ferguson, B. Shotorban, S. Mahalingam, Effects of distribution of bulk  
821 density and moisture content on shrub fires, *International Journal of Wildland Fire* 22 (2013)  
822 625-641.

- 823 [31] M.G. Etlinger, F.C. Beall, Development of a laboratory protocol for fire performance of  
824 landscape plants, *International Journal of Wildland Fire* 13 (2004) 479-488.
- 825 [32] G. Pellizzaro, P. Duce, A. Ventura, P. Zara, Seasonal variations of live moisture content  
826 and ignitability in shrubs of the Mediterranean Basin, *International Journal of Wildland Fire* 16  
827 (2007) 633-641.
- 828 [33] F.X. Jervis, G. Rein, Experimental study on the burning behaviour of *Pinus halepensis*  
829 needles using small-scale fire calorimetry of live, aged and dead samples, *Fire and Materials*  
830 40 (2016) 385-395.
- 831 [34] N. Bal, Forty years of material flammability: An appraisal of its role, its experimental  
832 determination and its modelling, *Fire Safety Journal* 96 (2018) 46-58.
- 833 [35] P.M. Fernandes, M.G. Cruz, Plant flammability experiments offer limited insight into  
834 vegetation–fire dynamics interactions, *New Phytologist* 194 (2012) 606-609.
- 835 [36] T. Barboni, L. Leonelli, P.-A. Santoni, V. Tihay-Felicelli, Influence of particle size on the  
836 heat release rate and smoke opacity during the burning of dead *Cistus* leaves and twigs, *Journal*  
837 *of Fire Sciences* 35 (2017) 259-283.
- 838 [37] J. Madrigal, C. Hernando, M. Guijarro, A new bench-scale methodology for evaluating the  
839 flammability of live forest fuels, *Journal of Fire Sciences* 31 (2013) 131-142.
- 840 [38] V. Tihay-Felicelli, P.-A. Santoni, T. Barboni, L. Leonelli, Autoignition of Dead Shrub  
841 Twigs: Influence of Diameter on Ignition, *Fire Technology* 52 (2016) 897-929.
- 842 [39] A.C. Dibble, R.H. White, P.K. Lebow, Combustion characteristics of north-eastern USA  
843 vegetation tested in the cone calorimeter: invasive versus non-invasive plants, *International*  
844 *Journal of Wildland Fire* 16 (2007) 426-443.
- 845 [40] S.V. Wyse, G.L.W. Perry, D.M. O’Connell, P.S. Holland, M.J. Wright, C.L. Hosted, S.L.  
846 Whitelock, I.J. Geary, K.J.L. Maurin, T.J. Curran, A quantitative assessment of shoot  
847 flammability for 60 tree and shrub species supports rankings based on expert opinion,  
848 *International Journal of Wildland Fire* 25 (2016) 466-477.
- 849 [41] G.H. Damant, S. Nurbakhsh, Christmas trees—what happens when they ignite?, *Fire and*  
850 *Materials* 18 (1994) 9-16.
- 851 [42] D. Stroup, L. DeLauter, J. Lee, G. Roadarmel, Scotch pine Christmas tree fire tests, Report  
852 of Test FR 4010. USDC, National Institute of Standards and Technology, Gaithersburg, MD, 1  
853 December 1999, 1999.
- 854 [43] V. Babrauskas, Chastagner G, S. E, Flammability of cut Christmas trees, IAAI Annual  
855 general meeting, Atlantic City, NJ, 2001, pp. 1–29.
- 856 [44] V. Babrauskas, Heat release rates, *The SFPE handbook of fire protection and engineering*,  
857 National Fire Protection Association, Quincy, MA, 2002, pp. 1–37.
- 858 [45] D.D. Evans, R.G. Rehm, E.S. Baker, *Physics-Based Modeling for WUI Fire Spread: Simplified Model Algorithm for Ignition of Structures by Burning Vegetation*, NIST Interagency/Internal Report (NISTIR) - 7179, NIST, Gaithersburg, MD, 2004.
- 861 [46] A. Long, B. Hinton, W. Zipperer, A. Hermansen-Baez, A. Maranghides, W. Mell, Quantifying and ranking the flammability of ornamental shrubs in the southern United States, Fire Ecology and Management Congress, The Association for Fire Ecology and Washington State University Extension, San Diego, CA, 2006, pp. 1-3.
- 865 [47] K. Zhou, J. Jia, J. Zhu, Experimental research on the burning behavior of dragon juniper tree, *Fire and Materials* 42 (2018) 173-182.
- 867 [48] E. Baker, J. Woycheese, Burning characteristics of Douglas-fir trees: scaling of individual tree fire based on tree size, Conference papers fire and materials, 2007, 10th international conference, Interscience Communications: London, San Francisco, CA, 2007.
- 870 [49] J. Li, S. Mahalingam, D.R. Weise, Experimental investigation of fire propagation in single live shrubs, *International Journal of Wildland Fire* 26 (2017) 58-70.
- 871

- 872 [50] R.H. White, D. DeMars, M. Bishop, Flammability of Christmas trees and other vegetation,  
873 in: C.J. Hilado (Ed.) Proceedings of the 24th international conference on fire safety, Columbus,  
874 OH, 1997, pp. 99-110.
- 875 [51] S.L. Stephens, D.A. Gordon, R.E. Martin, Combustibility of selected domestic vegetation  
876 subjected to desiccation, Proceedings of the 12th Conference on Fire and Fire Meteorology,  
877 Society of American Foresters: Bethesda, MD, Jekyll Island, GA, 1994, pp. 565–571.
- 878 [52] W. Tachajapong, J. Lozano, S. Mahalingam, D.R. Weise, Experimental modelling of  
879 crown fire initiation in open and closed shrubland systems, *International Journal of Wildland*  
880 *Fire* 23 (2014) 451-462.
- 881 [53] D. Prince, C. Shen, T. Fletcher, Semi-empirical Model for Fire Spread in Shrubs with  
882 Spatially-Defined Fuel Elements and Flames, *Fire Technology* 53 (2017) 1439-1469.
- 883 [54] C. Schemel, A. Simeoni, H. Biteau, J. Rivera, J. Torero, A calorimetric study of wildland  
884 fuels, *Experimental Thermal and Fluid Science* 32 (2008) 1381–1389.
- 885 [55] J. Madrigal, C. Hernando, M. Guijarro, C. Díez, E. Marino, A.J. De Castro, Evaluation of  
886 Forest Fuel Flammability and Combustion Properties with an Adapted Mass Loss Calorimeter  
887 Device, *Journal of Fire Sciences* 27 (2009) 323-342.
- 888 [56] P. Bartoli, A. Simeoni, H. Biteau, J.L. Torero, P.A. Santoni, Determination of the main  
889 parameters influencing forest fuel combustion dynamics, *Fire Safety Journal* 46 (2011) 27-33.
- 890 [57] A. Simeoni, J.C. Thomas, P. Bartoli, P. Borowieck, P. Reszka, F. Colella, P.A. Santoni,  
891 J.L. Torero, Flammability studies for wildland and wildland–urban interface fires applied to  
892 pine needles and solid polymers, *Fire Safety Journal* 54 (2012) 203-217.
- 893 [58] K. McGrattan, S. Hostikka, R. McDermott, J. Floyd, C. Weinschenk, K. Overholt, *Fire*  
894 *Dynamics Simulator User’s Guide*. Technical Report NIST Special Publication, 1019-6,  
895 National Institute of Standards and Technology, Gaithersburg, Maryland, 2013.
- 896 [59] N. Chiaramonti, E. Romagnoli, P.A. Santoni, T. Barboni, Comparison of the Combustion  
897 of Pine Species with Two Sizes of Calorimeter: 10 g vs. 100 g, *Fire Technology* 53 (2017) 741-  
898 770.
- 899 [60] S. Fehrmann, W. Jahn, J. de Dios Rivera, Permeability Comparison of Natural and  
900 Artificial *Pinus Radiata* Forest Litters, *Fire Technology* 53 (2017) 1291-1308.
- 901 [61] A. Ganteaume, M. Jappiot, T. Curt, C. Lampin, L. Borgniet, Flammability of litter sampled  
902 according to two different methods: comparison of results in laboratory experiments,  
903 *International Journal of Wildland Fire* 23 (2014) 1061-1075.
- 904 [62] S. Figueroa, J.d.D. Rivera, W. Jahn, Influence of Permeability on the Rate of Fire Spread  
905 over Natural and Artificial *Pinus radiata* Forest Litter, *Fire Technology*, doi:10.1007/s10694-  
906 019-00824-w(2019).
- 907 [63] S. Pyne, P. Andrews, R. Laven, *Introduction to Wildland Fire*, 2nd edition revised ed.,  
908 John Wiley & sons, inc., New York, 1996.
- 909 [64] D.W. Schwilk, Flammability Is a Niche Construction Trait: Canopy Architecture Affects  
910 Fire Intensity, *the american naturalist* 162 (2003) 725-733.
- 911 [65] A. Ganteaume, Does plant flammability differ between leaf and litter bed scale? Role of  
912 fuel characteristics and consequences for flammability assessment, *International Journal of*  
913 *Wildland Fire* 27 (2018) 342-352.
- 914 [66] M.G. Just, M.G. Hohmann, W.A. Hoffmann, Where fire stops: vegetation structure and  
915 microclimate influence fire spread along an ecotonal gradient, *Plant Ecology* 217 (2016) 631-  
916 644.
- 917 [67] H.E. Anderson, Relationship of fuel size and spacing to combustion characteristics of  
918 laboratory fuel cribs, Research Paper INT-424, USDA Forest Service, Intermountain Research  
919 Station, 1990.
- 920 [68] M.J. Gollner, Y. Xie, M. Lee, Y. Nakamura, A.S. Rangwala, Burning behavior of vertical  
921 matchstick arrays, *Comb. Sci. Tech.* 184 (2012) 585–607.

922 [69] M.F. Wolff, G.F. Carrier, F.E. Fendell, Wind-Aided Firespread Across Arrays of Discrete  
923 Fuel Elements. II. Experiment, *Combustion Science and Technology* 77 (1991) 261-289.

924 [70] W.R. Anderson, E.A. Catchpole, B.W. Butler, Convective heat transfer in fire spread  
925 through fine fuel beds, *International Journal of Wildland Fire* 19 (2010) 284-298.

926 [71] G.B. Peet, A fire danger rating and controlled burning guide for the Northern Jarrah (*Euc*  
927 *Marginata* sm) forest of Western Australia, Forests Dept, Perth, (1965).

928 [72] M.A. Finney, J.D. Cohen, J.M. Forthofer, S.S. McAllister, M.J.J. Gollner, D.J. Gorham,  
929 K. Saito, N.K. Akafuah, B.A. Adam, J.D. English, Role of buoyant flame dynamics in wildfire  
930 spread, *Proceedings of the National Academy of Sciences* 112 (2015) 9833-9838.

931 [73] N.D. Burrows, Flame residence times and rates of weight loss of eucalypt forest fuel  
932 particles, *International Journal of Wildland Fire* 10 (2001) 137-143.

933 [74] V. Babrauskas, R.D. Peacock, Heat release rate: the single most important variable in fire  
934 hazard, *Fire Saf. J.* 18 (1992) 255–272.

935 [75] J. Madrigal, M. Guijarro, C. Hernando, C. Díez, E. Marino, Estimation of Peak Heat  
936 Release Rate of a Forest Fuel Bed in Outdoor Laboratory Conditions, *Journal of Fire Sciences*  
937 29 (2011) 53-70.

938 [76] B. Porterie, J.L. Consalvi, A. Kaiss, J.C. Loraud, Predicting Wildland Fire Behavior and  
939 Emissions Using a Fine-Scale Physical Model, *Numerical Heat Transfer, Part A: Applications*  
940 47 (2005) 571-591.

941 [77] D. Morvan, J.L. Dupuy, F. Pimont, R.R. Linn, Numerical study of grassland fires  
942 behaviour using a physical multiphase formulation, *Forest Ecology and Management* 234  
943 (2006) S90-S90.

944 [78] S. Padhi, B. Shotorban, S. Mahalingam, Computational investigation of flame  
945 characteristics of a non-propagating shrub fire, *Fire Safety Journal* 81 (2016) 64-73.

946 [79] Y. Perez-Ramirez, W.E. Mell, P.A. Santoni, J.B. Tramoni, F. Bosseur, Examination of  
947 WFDS in Modeling Spreading Fires in a Furniture Calorimeter, *Fire Technology* 53 (2017)  
948 1795–1832.

949 [80] W. Mell, A. Maranghides, R. McDermott, S.L. Manzello, Numerical simulation and  
950 experiments of burning douglas fir trees, *Combustion and Flame* 156 (2009) 2023-2041.

951 [81] J.L. Dupuy, J. Maréchal, D. Morvan, Fires from a cylindrical forest fuel burner:  
952 combustion dynamics and flame properties, *Combustion and Flame* 135 (2003) 65-76.

953 [82] F. Pimont, J.L. Dupuy, R.R. Linn, Coupled slope and wind effects on fire spread with  
954 influences of fire size: a numerical study using FIRETEC, *International Journal of Wildland*  
955 *Fire* 21 (2012) 828-842.

956 [83] W. Mell, M.A. Jenkins, J. Gould, P. Cheney, A physics-based approach to modelling  
957 grassland fires, *International Journal of Wildland Fire* 16 (2007) 1-22.

958 [84] J. Dold, A. Simeoni, A. Zinoviev, R. Weber, The Palasca fire, September 2000: Eruption  
959 or Flashover?, in: D. Viegas (Ed.), *Forest Fire Accidents in Europe*, JRC, Ispra, 2009.

960 [85] S. Lahaye, J. Sharples, C. Hély, T. Curt, Toward safer firefighting strategies and tactics,  
961 *Toward safer firefighting strategies and tactics*, Imprensa da Universidade de Coimbra,  
962 Coimbra, 2018.

963 [86] C. Papió, L. Trabaud, Structural characteristics of fuel components of five Mediterranean  
964 shrubs, *Forest Ecology and Management* 35 (1990) 249-259.

965 [87] M. Cohen, E. Rigolot, M. Etienne, Modeling fuel distribution with cellular-automata for  
966 fuel-break assessment., in: D.X. Viegas (Ed.) *IV international conference on forest fire*  
967 *research*, Millpress, Rotterdam, Luso, Portugal, 2002.

968 [88] V. Krivtsov, O. Vigy, C. Legg, T. Curt, E. Rigolot, I. Lecomte, M. Jappiot, C. Lampin-  
969 Maillet, P. Fernandes, G.B. Pezzatti, Fuel modelling in terrestrial ecosystems: An overview in  
970 the context of the development of an object-orientated database for wild fire analysis,  
971 *Ecological Modelling* 220 (2009) 2915-2926.

- 972 [89] G. Heskestad, Similarity Relations for the Initial Convective Flow Generated by Fire, FM  
973 Report 72-WA/HT-17, Factory Mutual Research Corporation, Norwood, MA, 1972.
- 974 [90] K. Dungan, Performance-Based Approach to Designing and Analyzing Fire Detection  
975 Systems, NFPA 72® National Fire Alarm Code®, 2003.
- 976 [91] W.J. Parker, Calculations of the Heat Release Rate by Oxygen Consumption for Various  
977 Applications, *Journal of Fire Sciences* 2 (1984) 380–395.
- 978 [92] M.L. Janssens, Measuring Rate of Heat Release by Oxygen Consumption, *Fire Technol.*  
979 27 (1991) 234-249.
- 980 [93] F. Morandini, Y. Perez-Ramirez, V. Tihay, P.-A. Santoni, T. Barboni, Radiant, convective  
981 and heat release characterization of vegetation fire, *International Journal of Thermal Sciences*  
982 70 (2013) 83-91.
- 983 [94] F. Morandini, X. Silvani, Experimental investigation of the physical mechanisms  
984 governing the spread of wildfires, *International Journal of Wildland Fire* 19 (2010) 570-582.
- 985 [95] M.E. Alexander, M.G. Cruz, Assessing the effect of foliar moisture on the spread rate of  
986 crown fires, *International Journal of Wildland Fire* 22 (2013) 415-427.
- 987 [96] S. Fares, S. Bajocco, L. Salvati, N. Camarretta, J.-L. Dupuy, G. Xanthopoulos, M.  
988 Guijarro, J. Madrigal, C. Hernando, P. Corona, Characterizing potential wildland fire fuel in  
989 live vegetation in the Mediterranean region, *Annals of Forest Science* 74 (2017) 1.
- 990 [97] V. Babrauskas, Ignition handbook : principles and applications to fire safety engineering,  
991 fire investigation, risk management and forensic science, Fire Science Publishers, Issaquah,  
992 WA, 2003.
- 993 [98] NFPA92B, Guide for Smoke Management Systems in Malls, Atria, and Large Areas,  
994 National Fire Protection Association, Quincy, Massachusetts, 2000.
- 995 [99] A.M. Gill, P. Zylstra, Flammability of Australian forests, *Australian Forestry* 68 (2005)  
996 87-93.
- 997 [100] F. Pimont, J.-L. Dupuy, E. Rigolot, V. Prat, A. Piboule, Estimating Leaf Bulk Density  
998 Distribution in a Tree Canopy Using Terrestrial LiDAR and a Straightforward Calibration  
999 Procedure, *Remote Sensing* 7 (2015) 7995-8018.
- 1000 [101] P.M. Fernandes, W.R. Catchpole, F.C. Rego, Shrubland fire behaviour modelling with  
1001 microplot data, *Canadian Journal of Forest Research* 30 (2000) 889-899.
- 1002 [102] D. Morvan, J.L. Dupuy, Modeling of fire spread through a forest fuel bed using a  
1003 multiphase formulation, *Combustion and Flame* 127 (2001) 1981-1994.
- 1004

**Table 1:** Measurements of burning characteristics of whole plants in relation to some flammability components (TTI: Time to ignition; FD: Flame duration; HRR: Heat Release Rate; MLR: Mass Loss Rate; THR: Total Heat Released)

Vegetation species	Ignitability / ignition source	Sustainability	Combustibility	Consumability
[51] Tam junipers	- / 15 s natural gas wand	-	Peak HRR (kW)	-
[11] Gorse shrubs	TTI (s) / flame from pine wood	FD (s)	Rate of temperature increase ( $^{\circ}\text{C}\cdot\text{s}^{-1}$ ), HRR ( $\text{kW}\cdot\text{m}^{-2}$ ), MLR ( $\text{kg}\cdot\text{s}^{-1}$ )	Residual mass fraction (%)
[51] Christmas trees	- / paper match	FD (s)	Peak HRR (kW)	Mass consumed (kg, %)
[42] Scotch Pine Christmas trees	- / electric match	-	Peak HRR (kW)	Mass consumed (kg)
[43, 44] Christmas trees	- / small flame to a branch	-	HRR (kW)	-
[31] 6 species of landscape vegetation	- / propane burner	FD (s)	Peak HRR (kW)	Mass consumed (kg)
[50] Christmas trees and ornamental plants	TTI (s) / 8 s match, 20-30s lighter flame, 8 s electric arc, overheated wire	-	Peak HRR (kW)	-
[22] Small shrubs	- / propane burner		Peak HRR (kW)	Mass consumed (kg)
[45, 48] Douglas-fir trees	- / 5-15 s propane torch	FD (s)	Peak HRR (kW)	Mass consumed (kg)
[46] 34 species of ornamental shrubs	TTI (s) / 40 kW burner	FD (s)	Peak HRR (kW)	Mass loss (kg), canopy volume consumed ( $\text{m}^3$ )
[47] Dragon juniper trees	- / heptane ring fire	FD (s)	MLR ( $\text{kg}\cdot\text{s}^{-1}$ )	Mass consumed (%)
[49] Live shrubs	- / surface fire spreading	-	ROS ( $\text{m}\cdot\text{s}^{-1}$ ), MLR ( $\text{kg}\cdot\text{s}^{-1}$ )	Mass consumed (%)
[53] Branches of manzanita shrubs	- / flame from dry excelsior	FD (s)	-	Mass consumed (%)
[Present study] Shrubs of rockrose	TTI (s) / 20 kW/m <sup>2</sup> radiant panel	FD (s)	HRR (peak kW, growth rate $\text{kW}\cdot\text{s}^{-2}$ ), MLR ( $\text{g}\cdot\text{s}^{-1}$ )	Mass consumed (%), fuel consumption per particle class (%)



**Table 2:** Ambient conditions, plant sample characteristics and fire test properties

<b>Fire Test n°</b>	<b>Air Temp. (°C)</b>	<b>Air RH (%)</b>	<b>Shrub mass (kg)</b>	<b>Crown base height (m)</b>	<b>Total height (m)</b>	<b>Crown diameter (m)</b>	<b>Leaves MC (%)</b>	<b>0-2 MC (%)</b>	<b>Total Mass loss (kg)</b>	<b>THR (kJ)</b>
1	22.9	27.3	2.16	1.04	1.40	0.60	6	10	0.46	6426
2	23.5	26.0	1.50	0.90	1.35	0.60	6	10	0.49	4944
3	27.0	23.8	1.03	0.80	1.10	0.75	6	11	0.15	2368
4	26.0	41.0	1.68	0.95	1.20	0.60	14	31	0.37	4677
5	27.8	37.0	1.97	0.97	1.26	0.85	16	32	0.53	6293
6	25.5	43.4	2.02	0.93	1.31	0.62	15	30	0.38	4517
7	23.0	28.0	1.86	0.99	1.35	0.70	9	40	0.50	5527
8	22.0	31.0	2.30	1.02	1.25	0.74	9	41	0.81	11382
9	22.5	33.3	1.97	0.80	1.40	0.96	9	40	0.43	5730
10	20.9	45.0	2.99	1.00	1.25	0.64	18	44	0.47	6331
11	23.4	39.1	2.50	0.87	1.31	0.65	12	32	0.56	7115
12	23.9	38.7	2.39	0.89	1.25	0.58	12	32	0.81	11302
13	23.0	41.0	1.96	0.95	1.35	0.72	4	16	0.66	8190
14	23.0	43.0	2.39	0.90	1.20	0.75	8	25	0.49	6790
15	23.5	39.5	1.93	1.00	1.30	0.72	8	25	0.74	10579
16	24.8	38.2	0.93	0.85	1.15	0.60	8	25	0.39	6041
17	31.8	37.2	1.75	1.11	1.30	0.79	7	12	0.29	3317
18	31.2	38.2	2.12	0.90	1.32	0.70	5	10	0.31	3000
19	31.2	38.1	0.89	0.83	1.11	0.55	5	10	0.16	1802
20	26.0	45.0	2.23	1.10	1.30	0.65	17	30	0.49	5677
21	31.0	36.0	2.55	1.10	1.35	0.70	18	21	0.28	4605
22	28.0	39.5	2.30	1.15	1.35	0.60	9	18	0.60	7630
23	27.3	43.0	1.97	1.05	1.30	0.55	11	20	0.39	4486
24	27.3	42.8	1.86	1.00	1.20	0.70	13	24	0.59	6706
25	27.3	42.5	2.04	1.00	1.30	0.65	9	14	0.64	8632
26	30.5	36.5	1.83	1.00	1.30	0.69	12	16	0.50	6090
27	29.7	38.7	1.88	0.90	1.20	0.65	6	12	0.71	8730
28	30.0	38.0	2.17	1.05	1.30	0.76	6	7	0.36	4536

**Table 3:** Average fuel element properties for each class of particle used in WFDS (MC: moisture content;  $\sigma$ : surface area-to-volume ratio,  $\rho$ : density;  $\rho_b$ : bulk density)

	<b>Leaves</b>	<b>0-2 mm dead twigs</b>	<b>0-2 mm live twigs</b>	<b>2-4 mm live twigs</b>	<b>4-6 mm live twigs</b>	<b>6-25 mm live twigs</b>
MC (%)	7	2	23	27	35	45
$\sigma$ (m <sup>-1</sup> )	2081	1733	1733	1000	666	400
$\rho$ (kg.m <sup>-3</sup> )	478	961	961	961	961	961
$\rho_b(0.88 < z^* \leq 1.00)$ (kg.m <sup>-3</sup> )	3.99	0	1.63	0.04	0	0
$\rho_b(0.77 < z^* \leq 0.88)$ (kg.m <sup>-3</sup> )	2.73	0.13	2.45	0.99	0.08	0
$\rho_b(0.65 < z^* \leq 0.77)$ (kg.m <sup>-3</sup> )	1.32	0.31	2.79	2.34	1.07	0
$\rho_b(0.46 < z^* \leq 0.65)$ (kg.m <sup>-3</sup> )	0.52	1.04	1.09	2.46	2.95	0.37
$\rho_b(0.34 < z^* \leq 0.46)$ (kg.m <sup>-3</sup> )	0.48	1.04	0.49	2.13	3.83	3.54
$\rho_b(0.23 < z^* \leq 0.34)$ (kg.m <sup>-3</sup> )	0.30	0.38	1.18	1.41	2.48	12.27
$\rho_b(0.00 < z^* \leq 0.23)$ (kg.m <sup>-3</sup> )	0	0	0	N/A	N/A	N/A

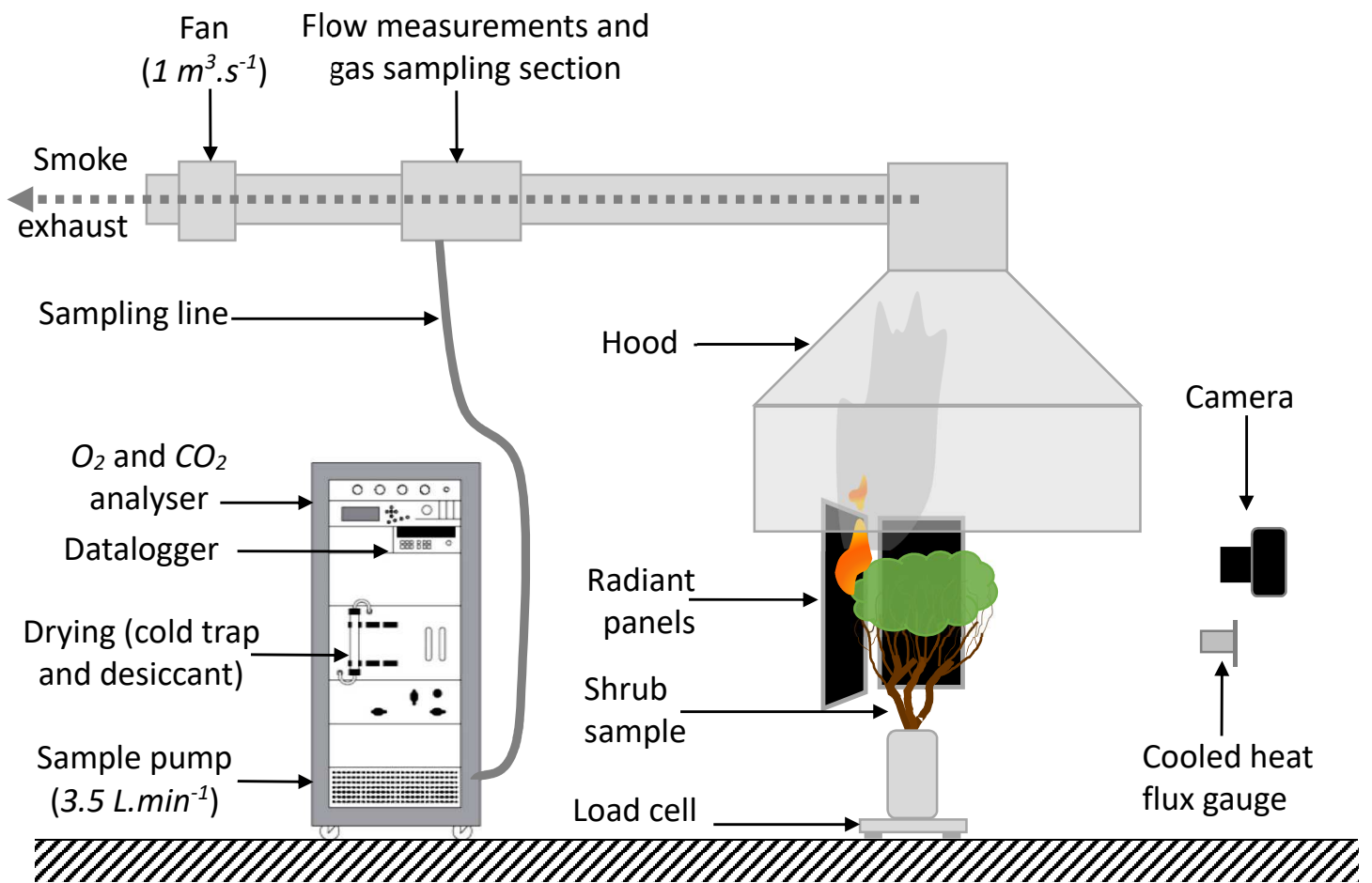


**Fig. 1.** Layout of the experimental setup

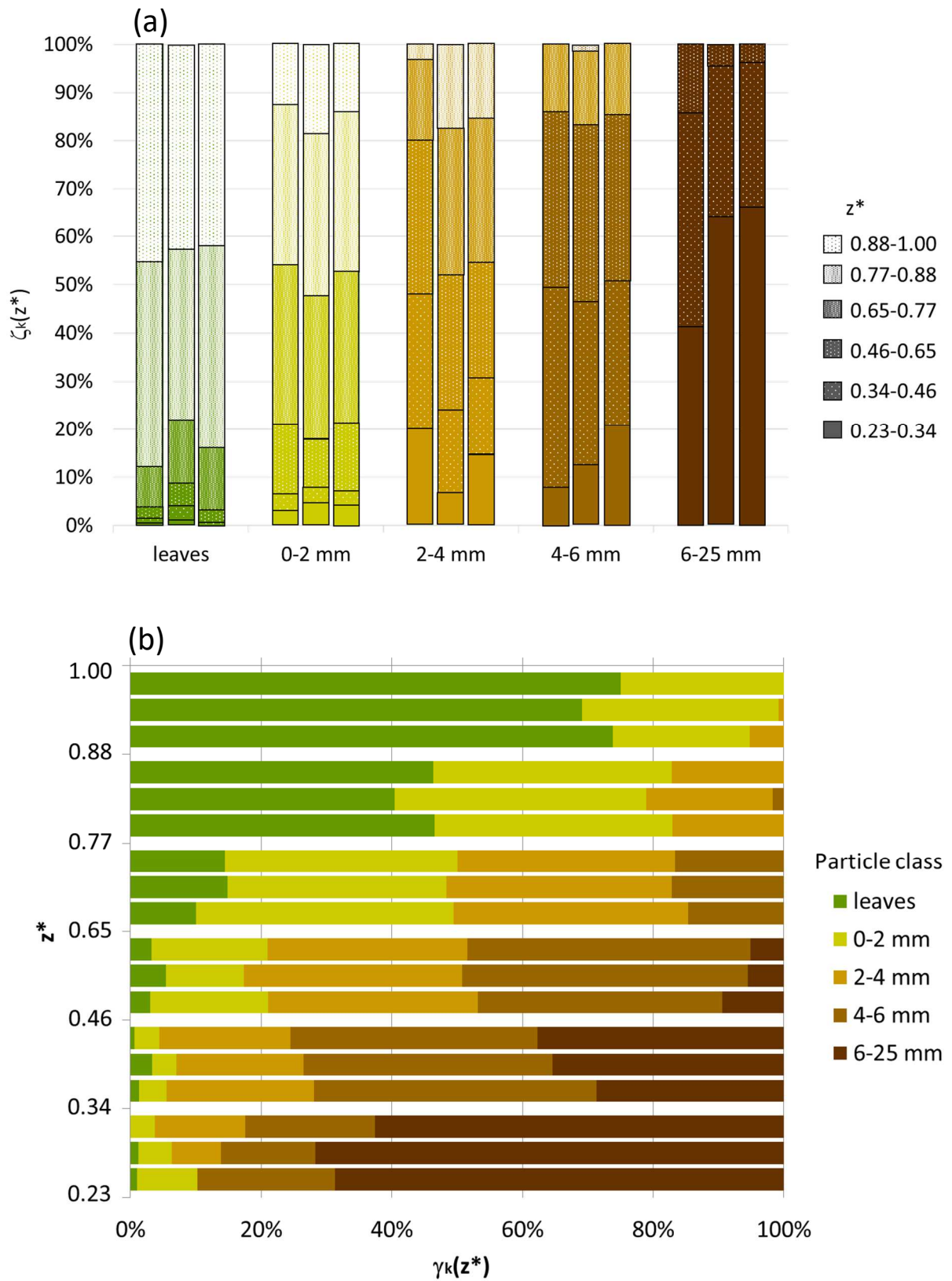


**Fig. 2.** Characterization of 3 shrubs of rockrose (a) mass distribution of the different particle size classes as function of non-dimensional height  $z^*$  and (b) mass fraction versus height for the different particle size classes

Ignitability: TTI

Combustibility: Fire growth parameter, HRR, MLR

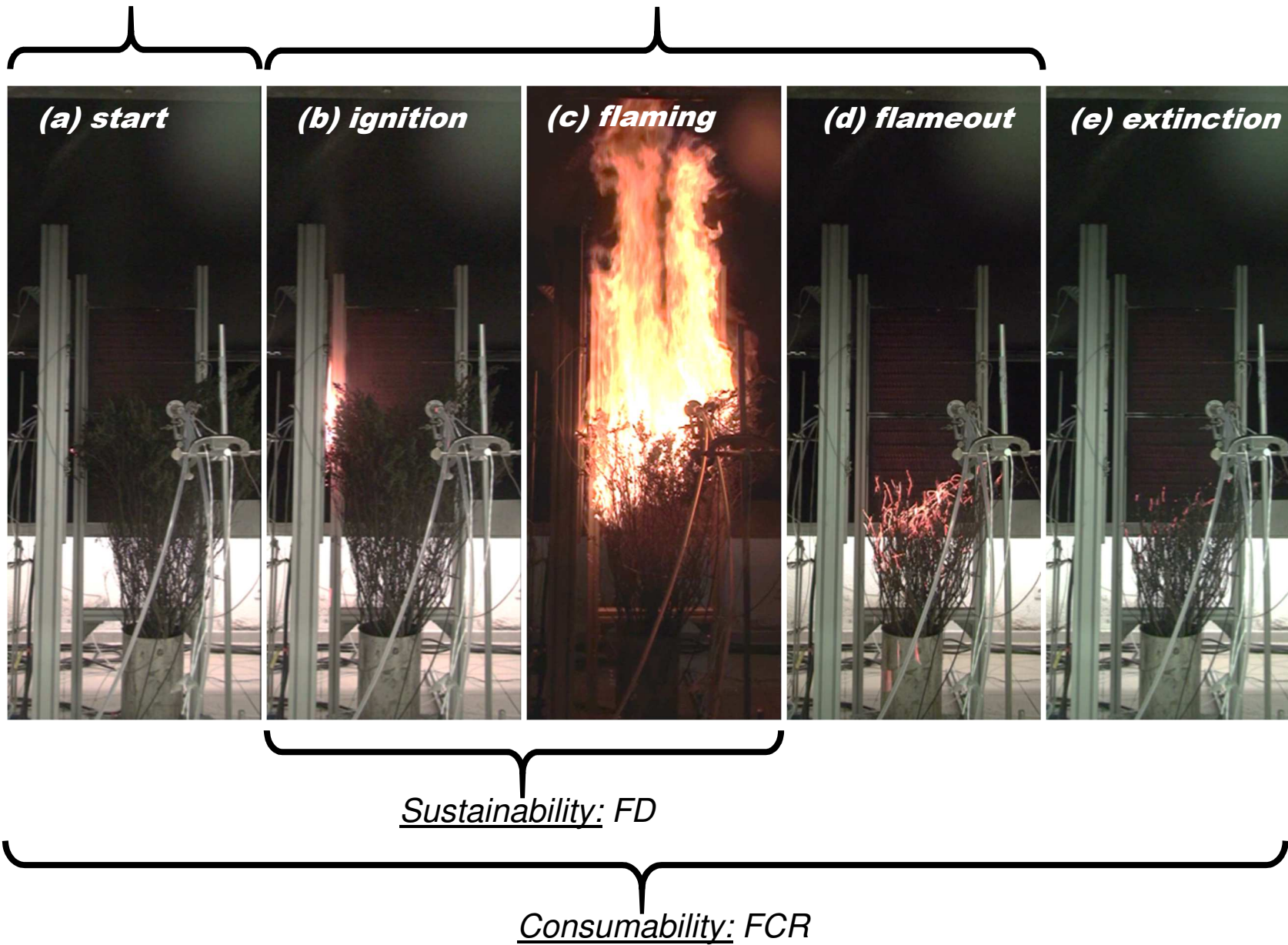


**Fig. 3.** Measurements of the 4 components of flammability during the different combustion process phases: (a) test start, (b) ignition, (c) flaming, (d) flameout and char oxidation, (e) extinction

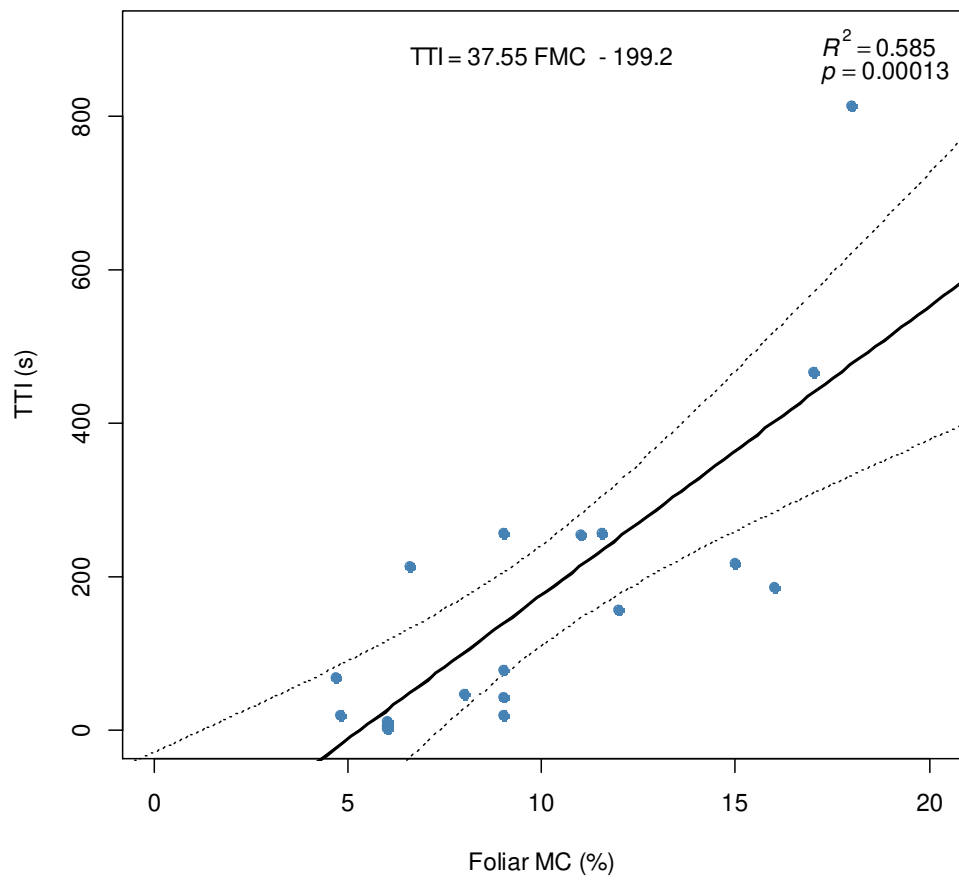


**Fig. 4.** Influence of foliar MC on ignitability

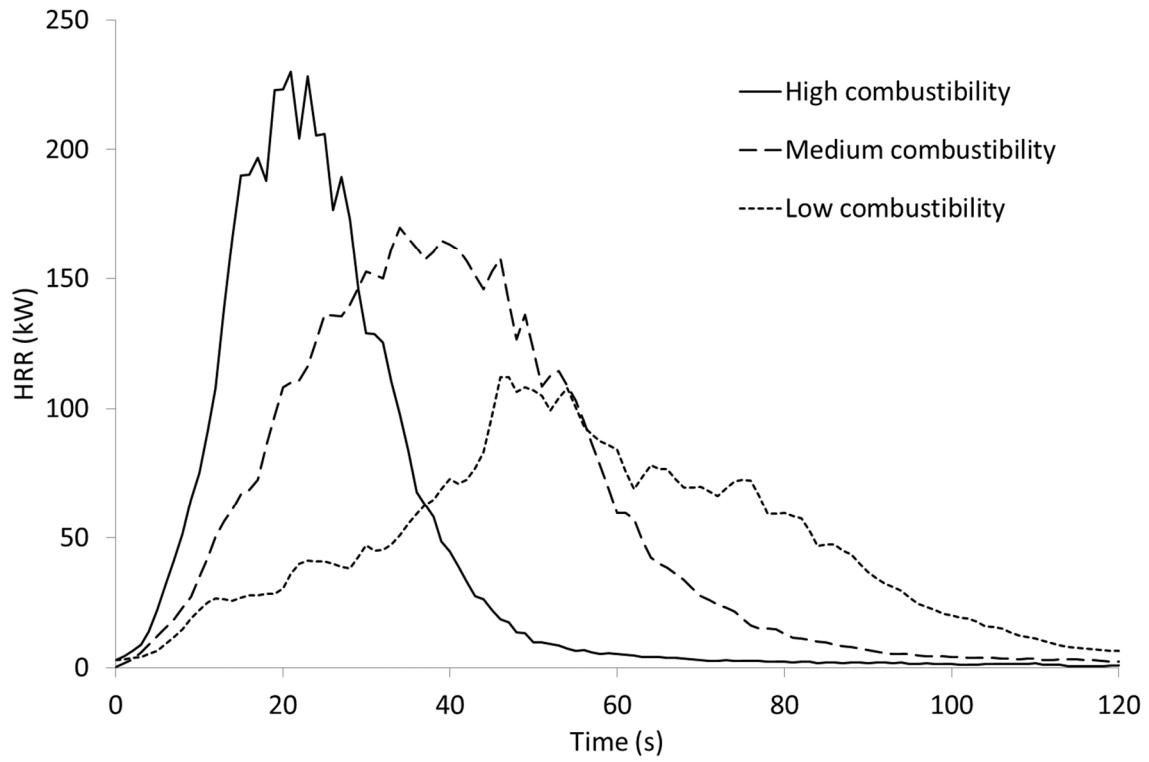


**Fig. 5.** Examples of HRR after TTI versus time corresponding to low ( $\alpha = 0.10 \text{ kW}\cdot\text{s}^{-2}$ ) medium ( $\alpha = 0.22 \text{ kW}\cdot\text{s}^{-2}$ ) and high combustibility ( $\alpha = 0.52 \text{ kW}\cdot\text{s}^{-2}$ ) for fire tests 4, 14 and 15, respectively



**Fig. 6.** Fire growth observed 30 s after ignition for different values of  $\alpha$ : (a) low combustibility:  $\alpha = 0.10 \text{ kW}\cdot\text{s}^{-2}$  (fire test 4); (b) medium combustibility:  $\alpha = 0.22 \text{ kW}\cdot\text{s}^{-2}$  (fire test 14) and (c) high combustibility:  $\alpha = 0.52 \text{ kW}\cdot\text{s}^{-2}$  (fire test 15)



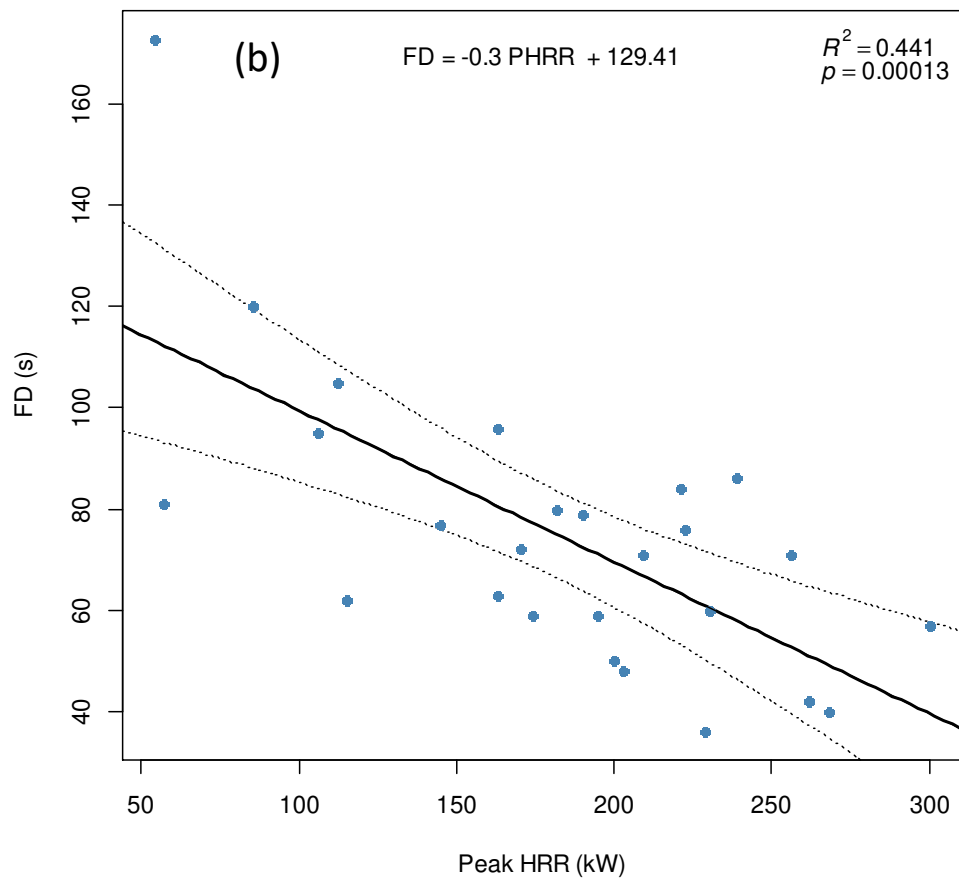
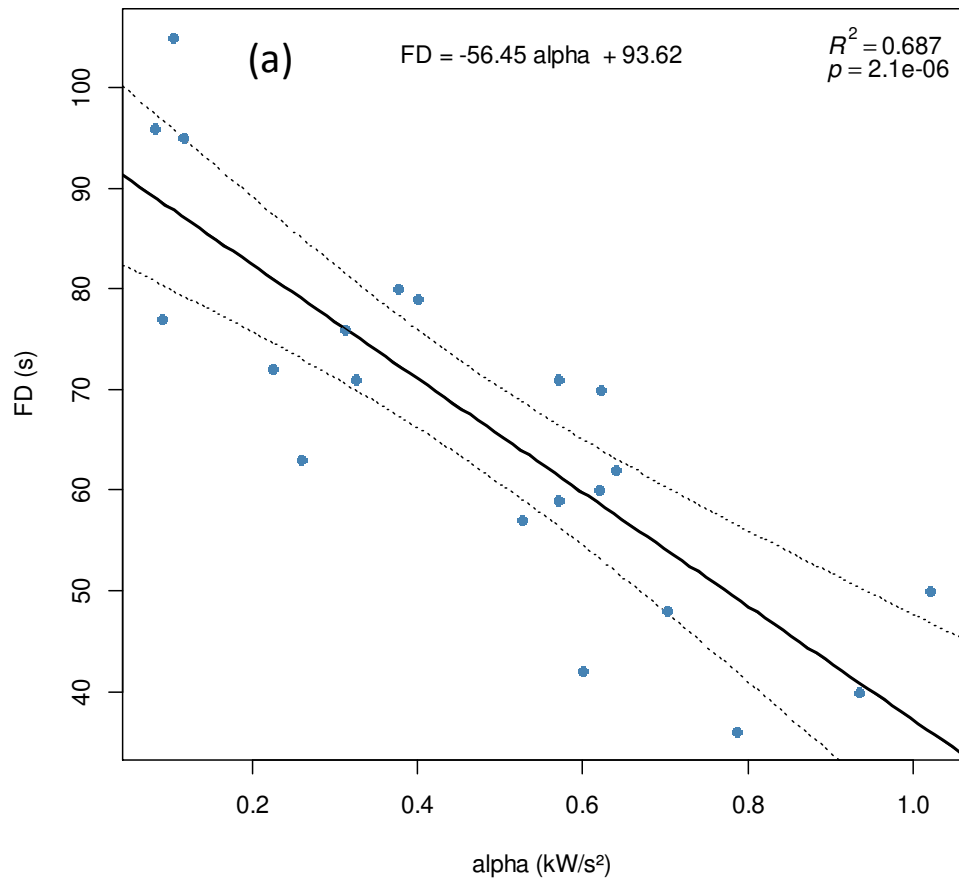


**Fig. 7.** Relationship between sustainability and combustibility (a) Flame duration FD (s) versus fire growth parameter  $\alpha$  (kW.s<sup>-2</sup>) and (b) Flame duration FD (s) versus peak HRR (kW)

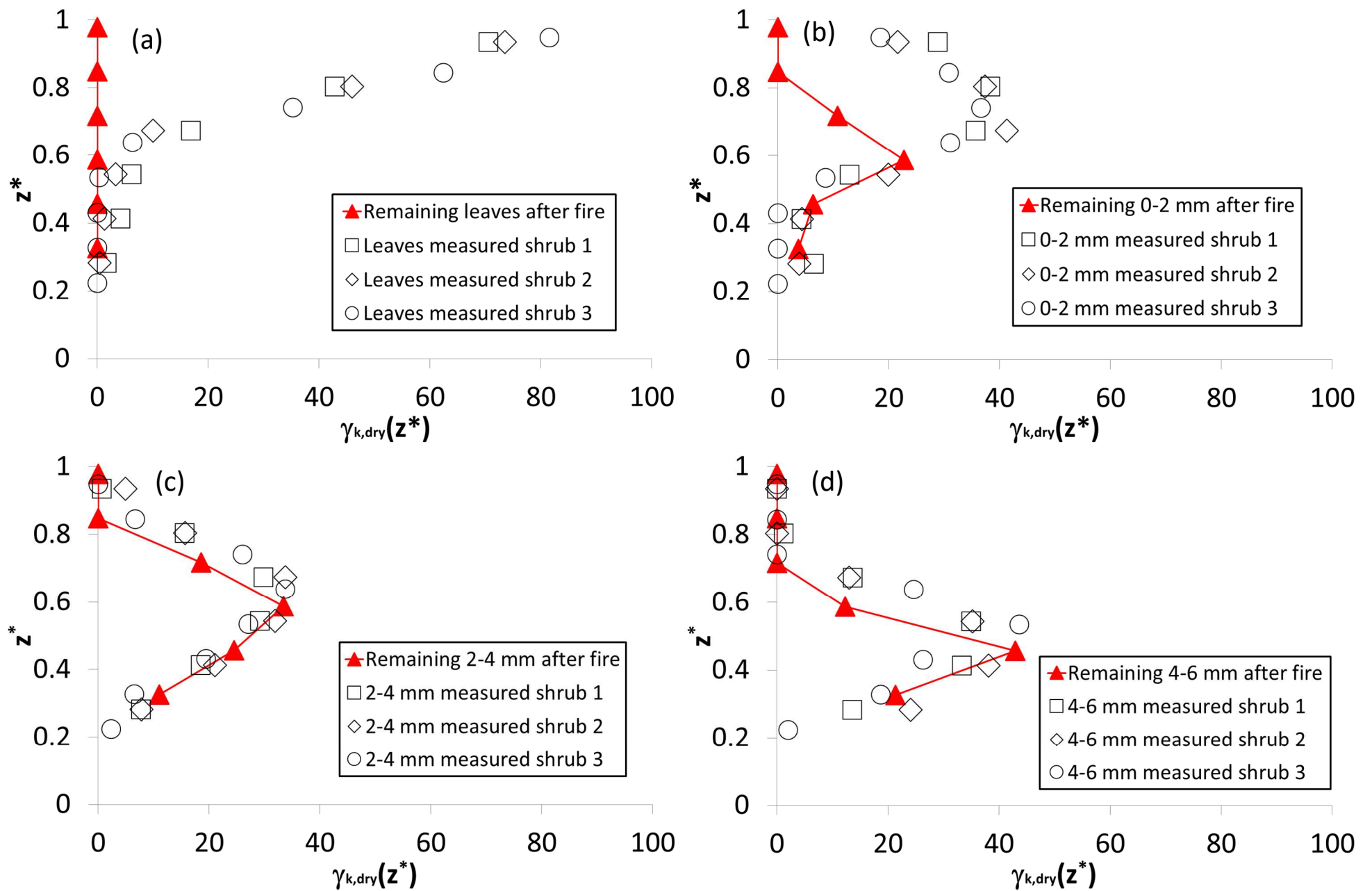


**Fig. 8.** Characterization of the fuel consumption at particle level: comparison of the mass fraction before (from the destructive measurements of 3 shrub samples) and after the burning (fire test 15), for the different particles size classes: (a) leaves, (b) twigs of 0-2 mm diameter, (c) twigs of 2-4 mm diameter and (d) twigs of 4-6 mm diameter.

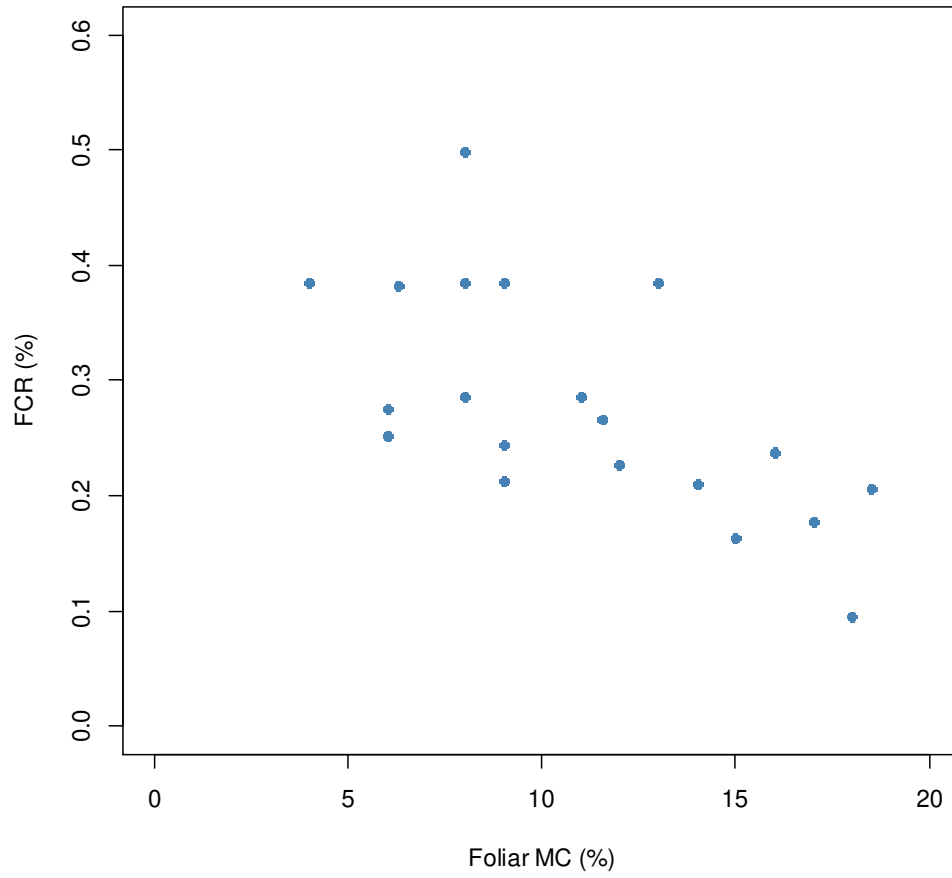


**Fig. 9.** Fuel consumption ratio versus foliar moisture content

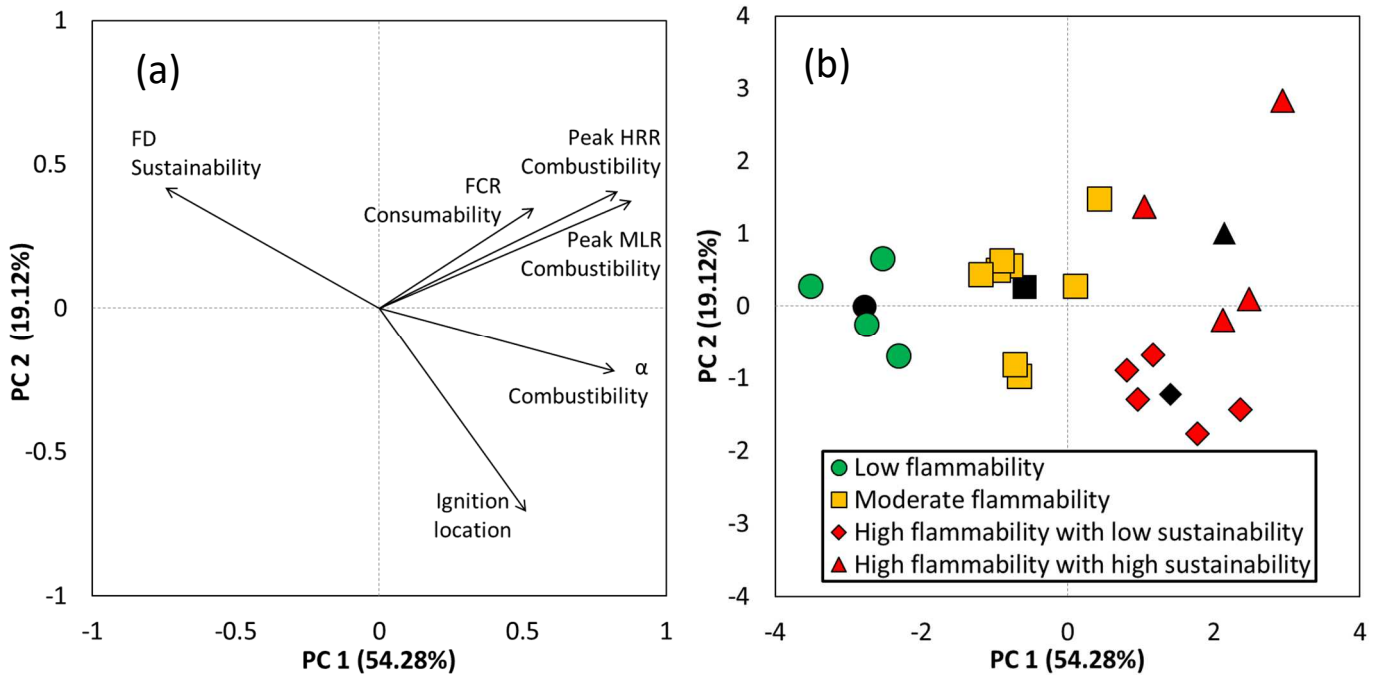


**Fig. 10.** (a) Principal Component Analysis of flammability variables and (b) Projection of the fire tests on the factorial plane for PC 1 and PC 2 (for each flammability group (circle, square, triangle and diamond), the color and black markers refer to single experiment and barycenter of the corresponding flammability group, respectively)

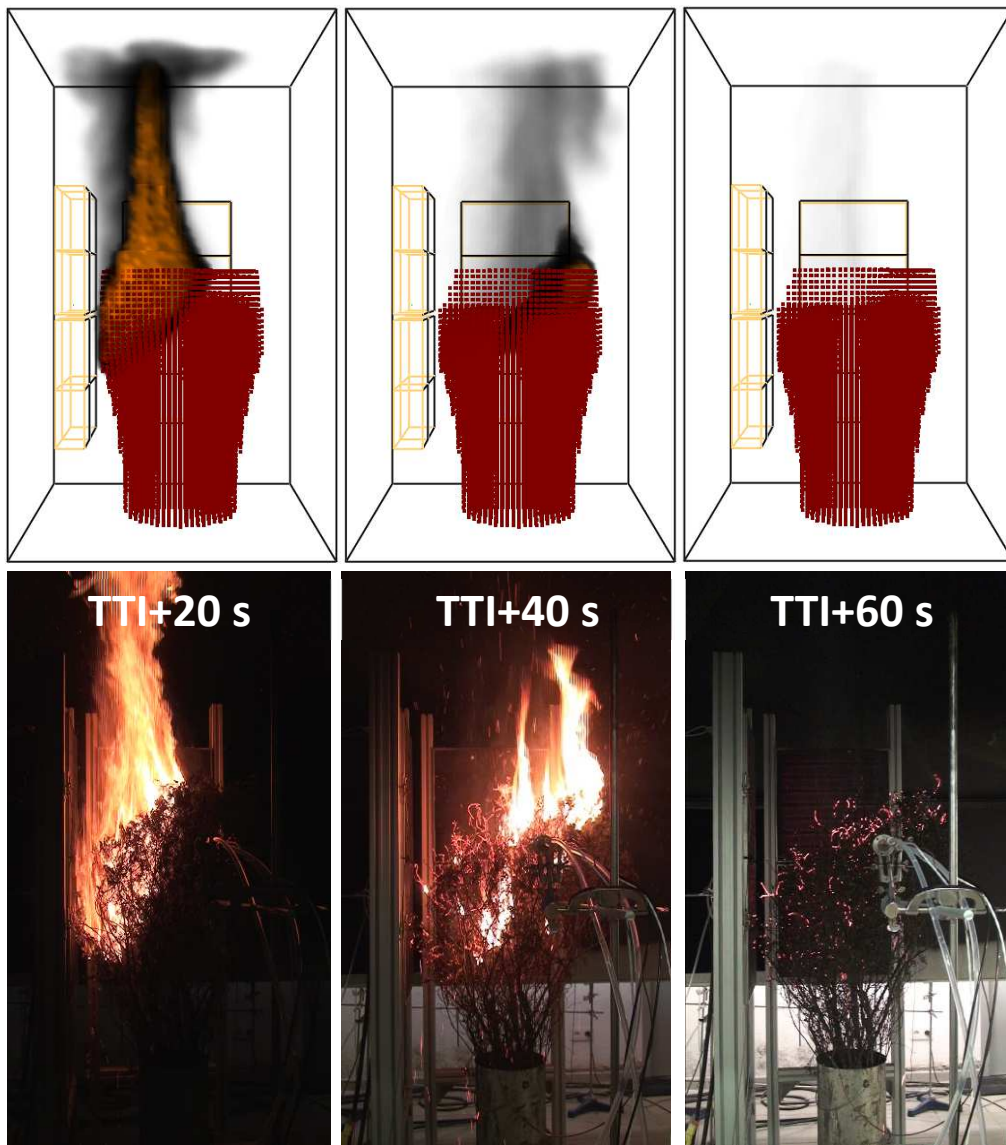


**Fig. 11.** Comparison of the predicted ( $200 \text{ kW/m}^3$  isocontour) and observed (test 15) fire spread over time

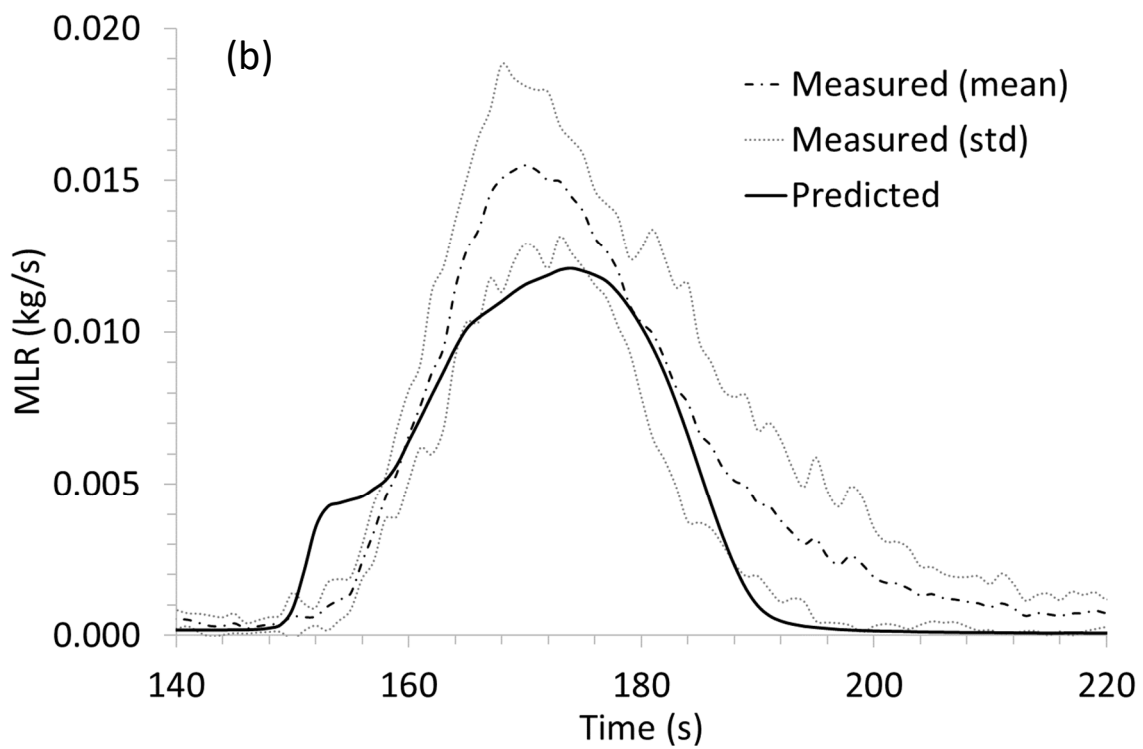
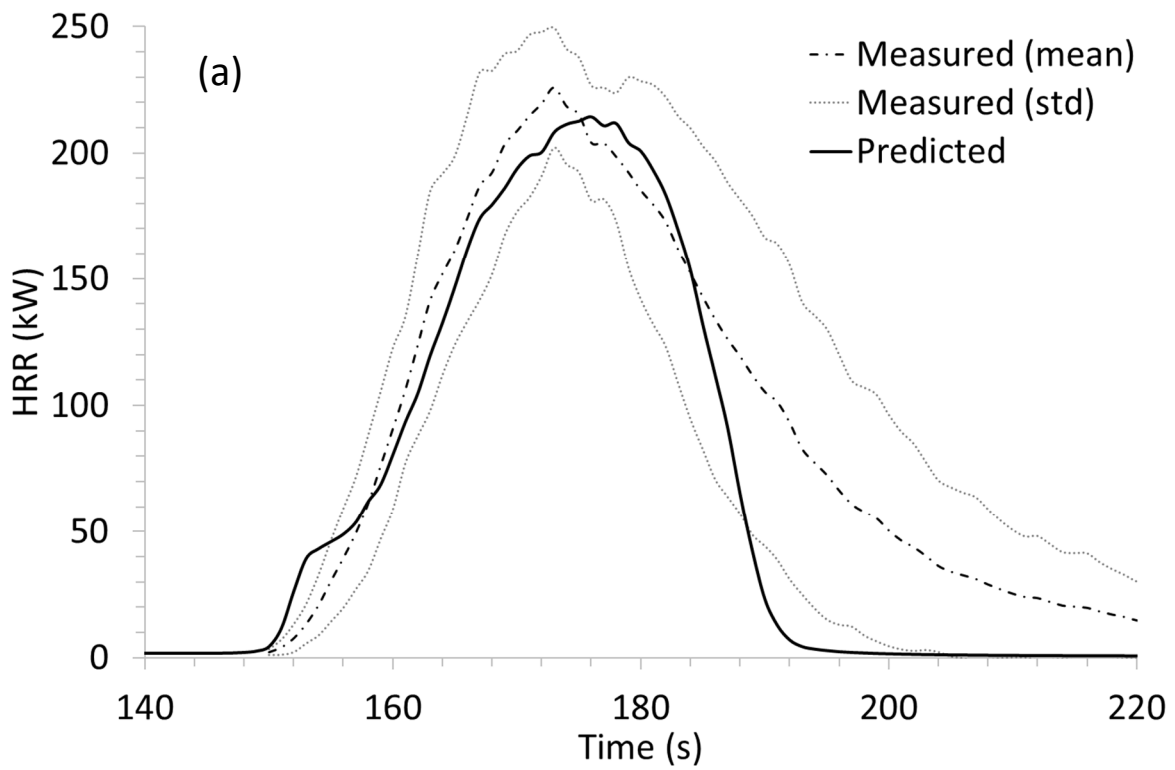
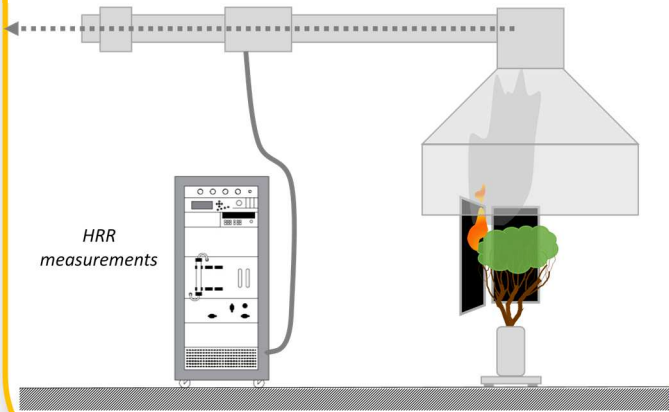


**Fig. 12.** Comparison of the predictions and measurements (a) HRR and (b) MLR. The experimental data are obtained from the mean (and standard deviation) of 5 fire tests corresponding to the high flammability with low sustainability regime

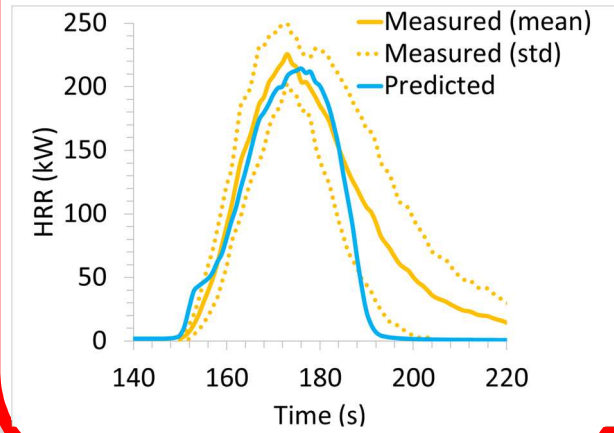
## Large-scale calorimeter



## Flammability



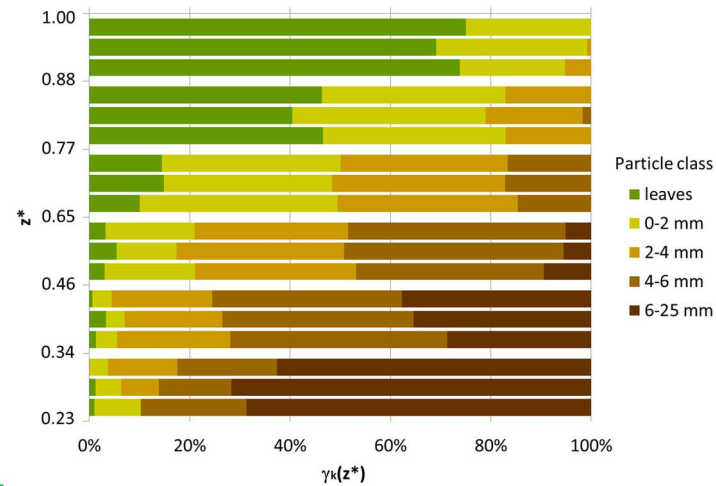
## Model evaluation



## Full-scale plant



## Fuel elements characterization



## WFDS simulation

